Verification and Intercomparison of Multimodel Simulated Land Surface Hydrological Datasets over the United States

YUN FAN, HUUG M. VAN DEN DOOL, AND WANRU WU

NOAA/NWS/NCEP/Climate Prediction Center, Camp Springs, Maryland

(Manuscript received 12 May 2010, in final form 20 January 2011)

ABSTRACT

Several land surface datasets, such as the observed Illinois soil moisture dataset; three retrospective offline run datasets from the Noah land surface model (LSM), Variable Infiltration Capacity (VIC) LSM, and Climate Prediction Center leaky bucket soil model; and three reanalysis datasets (North American Regional Reanalysis, NCEP/Department of Energy Global Reanalysis, and 40-yr ECMWF Re-Analysis), are used to study the spatial and temporal variability of soil moisture and its response to the major components of land surface hydrologic cycles: precipitation, evaporation, and runoff. Detailed analysis was performed on the evolution of the soil moisture vertical profile. Over Illinois, model simulations are compared to observations, but for the United States as a whole some impressions can be gained by comparing the multiple soil moisture–precipitation–evaporation–runoff datasets to one another. The magnitudes and partitioning of major land surface water balance components on seasonal–interannual time scales have been explored. It appears that evaporation has the most prominent annual cycle but its interannual variability is relatively small. For other water balance components, such as precipitation, runoff, and surface water storage change, the amplitudes of their annual cycles and interannual variations are comparable. This study indicates that all models have a certain capability to reproduce observed soil moisture variability on seasonal–interannual time scales, but offline runs are decidedly better than reanalyses (in terms of validation against observations) and more highly correlated to one another (in terms of intercomparison) in general. However, noticeable differences are also observed, such as the degree of simulated drought severity and the locations affected—this is due to the uncertainty in model physics, input forcing, and mode of running (interactive or offline), which continue to be major issues for land surface modeling.

1. Introduction

The land surface process is one of the most important components of the earth's weather and climate system. Among many land surface variables, soil moisture, snowpack, and deep-layer soil temperature often have a longer memory than the fast changing weather systems. It is also well known that these land surface variables can influence the partitioning of water and energy fluxes at the land surface, and thereby impact the overlying atmosphere through sensible and latent heat exchanges, as well as by changing land surface albedo. The importance of land surface memory is considered second to the sea surface temperature (SST) and has attracted considerable research interests for quite a long time (Reed 1925; Namias 1952; Mahrt and Pan 1984; Delworth and Manabe 1988; Yeh 1989; Huang and Van den Dool 1993; Fennessy and Shukla 1999; Dirmeyer 2000; Koster and Suarez 2001; Koster et al. 2003; Wu et al. 2002; Vautard et al. 2007; Van den Dool 2007). Many studies indicate significant impacts from antecedent soil moisture conditions on monthly–seasonal near-surface climate predictability, at least during the warm season. Accurately representing soil moisture is thus critically important, not only important for meteorology, but also for hydrology, agriculture, environment, etc.

During the last two decades, our knowledge about land surface and atmosphere interaction has been greatly improved and several Land Data Assimilation System (LDAS) projects (Van den Hurk 2002; Mitchell et al. 2004b; Rodell et al. 2004; Dirmeyer et al. 2006) have been developed. However, many important scientific issues or questions are still not fully resolved and need further investigation, such as the quantitative understanding of the land surface water and energy budgets on the global and continental scales (Roads et al. 2003) and nonlocal impacts

Corresponding author address: Dr. Yun Fan, Climate Prediction Center, 5200 Auth Road, Rm. 806, Camps Springs, MD 20746.
E-mail: yun.fan@noaa.gov

DOI: 10.1175/2011JHM1317.1

of soil moisture on the weather and climate (Van den Dool et al. 2003; Zhang and Frederikson 2003). This is mainly due to a lack of sufficient observations for all water and energy balance components but also to the difficulties of analyzing the problems. Although there are some very limited networks that have routine observations for one–two decades in different places (Robock et al. 2000), long-term, routine, and global-scale in situ observational networks for land surface variables are not yet established. The National Soil Climate Analysis Network (SCAN) (Schaefer and Paetzold 2001) has relatively good network coverage over the United States. However, the data density, quality, and time duration vary greatly with location and many stations do not have a long continuous history. Analyzing the data from SCAN on continental scales still faces big challenges.

Satellite-based remote sensing of soil moisture is promising but still immature. Most traditional (radiation based) satellites can only sense soil moisture effectively in the upper few centimeters of the soil layer over sparsely vegetated areas. Therefore, it gives little memory information about deeper soil layers and limits its usefulness for medium- to long-term prediction. The Gravity Recovery and Climate Experiment (GRACE) twin satellites, launched in March 2002, can make more detailed and precise measurements of the change of the earth's gravity field—the mass movement around the earth. Hence, they can indirectly detect the land surface water storage changes in deeper soil layers. Some preliminary comparisons between calculated soil moisture and the GRACE satellite data are very encouraging and show potential (Wahr et al. 2004; Van den Dool et al. 2004).

So far, most soil moisture datasets used in both research and weather and climate predictions are ''calculated'' soil moisture, because no observed soil moisture data have been assimilated into these land surface analysis systems. They are either from the National Centers for Environmental Prediction–National Center for Atmospheric Research (NCEP–NCAR) Global Reanalysis 1 (R1; Kalnay et al. 1996; Kistler et al. 2001), NCEP/Department of Energy Global Reanalysis 2 (R2; Kanamitsu et al. 2002), 40-yr European Centre for Medium-Range Weather Forecasts (ECMWF) Re-Analysis (ERA-40; Uppala et al. 2005), and North American Regional Reanalysis (RR; Mesinger et al. 2006), or the offline runs of land surface models (LSMs), sometimes called land surface data assimilation systems (Maurer et al. 2002; Van den Hurk 2002; Dirmeyer et al. 2004; Mitchell et al. 2004b; Rodell et al. 2004; Fan et al. 2006). The quality of these calculated soil moisture datasets crucially depends on the quality of input forcing data and land surface models used. Previous research (Maurer et al. 2001; Kanamitsu et al. 2003; Dirmeyer et al. 2004; Fan and Van den Dool 2005) and this paper show that the quality of soil moisture datasets from the global reanalyses is not very good, when compared to the limited observations. The widespread biases in simulated precipitation, surface air temperature, and surface radiation fields may be the main reason. Without suitable negative feedbacks, these biases can drive calculated soil moisture far away from realistic values.

In recent years, the research activities from the Global Energy and Water Cycle Experiment (GEWEX) Continental-Scale International Project (GCIP), the Coordinated Enhanced Observing Periods (CEOP) project, and the Climate Prediction Project for the Americas (CPPA) have further improved our understanding of land surface processes. Benefitting from more accurate input forcing and modeling improvements (such as using better observed precipitation, bias correction techniques, elevation adjustments, and improved land surface models), land surface simulation from the offline runs, such as some National LDAS (NLDAS) runs and the North America Regional Reanalysis (Mesinger et al. 2006), shows clear and indisputable improvements (Maurer et al. 2002; Fan and Van den Dool 2005; Fan et al. 2006) over the older global reanalyses.

Because of features of some land surface datasets used here, the spatial domain of this study will be constrained to the contiguous United States (CONUS). This paper will focus on the following questions: What are the skills for most of the currently existing soil moisture datasets, when compared to limited observations? What are the main statistical features of spatial–temporal distributions of these existing land surface datasets? Can these land surface datasets capture the high-impact hydrological events, such as the worst droughts and floods over the CONUS, and what do the spatial structures of those hydrological extreme events look like? Where do some problems (e.g., completely missing or overestimating targets) come from and what are the possible reasons? The paper is organized as follows: section 2 describes seven land surface datasets used in this study. Section 3 presents the annual cycles and long-term variability of observed and simulated soil moisture datasets, simulated land surface water budget components over Illinois. The statistical features and differences of the simulated land surface variables over the entire United States are given in section 4. Conclusions and the discussion are provided in section 5.

2. Data description

Seven land surface datasets are used in this study, including one observational dataset, three ''offline'' model runs, and three reanalysis datasets. These datasets are

used to study the spatial and temporal variability of soil moisture and its relation to the major components of land surface hydrology: precipitation, evaporation, and runoff. The period for each dataset may differ, but in any comparison we use the common years; for instance, when the observation is involved, the comparison period spans from 1984 to 1999, while model-based intercomparison covers the period 1980–99. The resolution of each dataset is different, and in various figures we use the highest resolution for each model, but when correlating datasets we use a common grid. In all cases we deal with monthly mean or monthly accumulated data. Detailed information about these datasets is as follows.

a. Observed Illinois soil moisture dataset (1981–2004)

So far, in the United States, the Illinois observation network provides probably the best long-term series (1981–present) of routine soil moisture observations from 18 sites throughout the state of Illinois (Hollinger and Isard 1994). The instantaneous observations are made about twice each month and measured for the top 10 cm of soil, and then for 10 more layers (e.g., 10–30, 30–50, 50–70, 70–90, 90–110, 110–130, 130–150, 150–170, 170–190, and 190–200 cm) down to a depth of 2 m. The vegetation at all stations is grass, except for one station with bare soil that is collocated with a grass-covered station. The above dataset was converted to a monthly mean dataset by averaging the measurements made per month. The first 3 yr of data are clearly inconsistent with the observation made after 1983, because of changing observational instruments. Therefore, in most cases the observed Illinois soil moisture data used in this study is for 1984–2003, if not mentioned otherwise. The dataset is available from the Global Soil Moisture Data Bank (Robock et al. 2000).

b. Noah LSM retrospective NLDAS run (1948–present)

The Noah LSM is the current operational land surface model used at NCEP in most numerical weather and climate models. It originated from a physically based soil–vegetation–atmosphere transfer (SVAT) scheme (Mahrt and Pan 1984), often referred to as the Oregon State University (OSU) LSM. During the past 10 years, the Noah LSM was jointly developed under multi-institute projects and underwent substantial upgrades, such as more soil layers (from two to four layers), improved canopy conductance and bare soil evaporation treatments, and updated cold season physics (Ek et al. 2003; Mitchell et al. 2004b). These improvements significantly enhanced the Noah LSM capability to simulate more realistic land surface hydrological processes (Mitchell et al. 2004b; Ek et al. 2003; Fan et al. 2006). The Noah LSM's four soil layers have 10-, 30-, 60-, and 100-cm depths respectively, yielding a total depth of 2 m, with the root zone spanning the top three (four) layers for nonforest (forest) vegetation classes. The model was configured on the NLDAS grid at $0.125° \times 0.125°$ horizontal resolution. Further details on the Noah model and the NLDAS configuration can be found in Mitchell et al. (2004b).

To run the Noah LSM retrospectively for greater than 50 years, the quality of the required 7-hourly land surface meteorological forcing variables at $\frac{1}{8}°$ spatial resolution is critically important for the output of the land surface model. Some unique procedures and techniques were developed to prepare this forcing dataset, such as solar zenith angle diurnal adjustment for surface downward shortwave radiation and elevation adjustment to 2-m air temperature, surface pressure, downward longwave radiation, and 2-m specific humidity, and disaggregation of the observed daily precipitation (based on thousands of gauges) with the help of observed hourly precipitation (having far fewer gauges). The output of the Noah LSM includes all water and energy budget components. More detailed information about this retrospective run can be found in Fan et al. (2006).

c. VIC LSM retrospective NLDAS run (1950–2000)

The Variable Infiltration Capacity (VIC) LSM (Liang et al. 1994) is a macroscale hydrologic model that solves full water and energy balances as does the Noah LSM. It currently also runs in parallel with the Noah LSM in real-time forward mode at NCEP. The VIC LSM is also forced with seven surface meteorological variables: precipitation, temperature, wind, surface air humidity, downward longwave and shortwave radiation, and surface air pressure. The VIC LSM used here has three vertical layers and the soil depths in the VIC LSM grid cells vary between 1.0 and 2.3 m. The VIC retrospective run (Maurer et al. 2002) was also configured on the same NLDAS grid as the Noah LSM described above and it covered the period from 1950 to the middle of 2000. This retrospective run used observed daily precipitation, daily temperature, and temperature range to derive other needed forcing fields (excluding wind) with certain established relationships, such as empirically linking radiation to the difference of maximum and minimum temperatures. The wind fields are obtained from the R1 10-m wind fields regridded to the NLDAS grid. The outputs of the VIC LSM include all water and energy budget components in 3-hourly temporal resolution as well as a daily summary. The soil moisture tendency and snow water tendency are derived as monthly averages.

d. Soil moisture datasets from the CPC leaky bucket model (1948–present)

The Climate Prediction Center (CPC) leaky bucket soil moisture model (hereafter LB) was developed in the mid-1990s (Huang et al. 1996). The land surface variables are estimated by a one-layer simple hydrological model. The model was tuned to the runoff of several small river basins in eastern Oklahoma resulting in a maximum holding capacity of 760 mm of water. Along with a common porosity of 0.47 this implies a soil column of 1.6 m. The model only takes precipitation and temperature as forcing variables and calculates soil moisture, evaporation and runoff. The potential evaporation is estimated from observed temperature. The original dataset is for the 344 U.S. climate divisions and is available for the period from 1931 to present. A global LB version, including the United States, is on a 0.5° resolution and is forced with observed CPC gauge-based global land surface precipitation (Chen et al. 2002) and CPC observation-based global land surface temperature covering the period of 1948–present (Fan and Van den Dool 2004, 2008). A strong, or noteworthy, point about LB is that it produces considerable runoff—many land surface models used in meteorology tended (and tend) to produce high evaporation and very little runoff.

e. R2 (1979–present)

The R1 was the first generation of global atmosphere–land reanalyses released to the public in the mid-1990s (Kalnay et al. 1996; Kistler et al. 2001). It includes the most comprehensive atmospheric and land surface hydrology dataset at that time and covers the time period from 1948 to present. In R1, an artificial nudging term was used to avoid drift too far away from the prescribed soil moisture climatology. The R2 (Kanamitsu et al. 2002) is a follow-up to the R1. It corrected some known errors in the R1 and used updated model physics, updated data assimilation system, improved fixed field inputs, and diagnostic outputs. Importantly the soil moisture nudging term was removed in the R2 and the differences between model-generated and observed precipitation are used (with a 5-day delay) to adjust the calculated soil moisture. Therefore, the R2 can be viewed as an updated version of the R1 and both of them are widely used in research and climate monitoring. The land model used in both R1 and R2 is the two-layer OSU LSM (Pan and Mahrt 1987). In this study, the R2 dataset will be used unless stated otherwise. The horizontal resolution, corresponding to T62 Gaussian resolution, is about 2.0° × 2.0°.

f. RR (1979–present)

Based on the R1 and the R2 experience, the North American Regional Reanalysis (Mesinger et al. 2006) was developed about 10 years later with the operational regional NCEP Eta Model, a further updated data assimilation system, a more advanced Noah land surface model (Mitchell et al. 2004a), further improved input datasets, and using the R2 to provide lateral boundary conditions. In particular, the RR has successfully assimilated the high-quality (hourly 32-km resolution) observed precipitation [same as the one used in the above Noah NLDAS (section 2b) retrospective run] into the atmospheric analysis. Precipitation is one of the most important forcing fields to the land surface hydrological processes. Thus, in principle, the outputs from the land surface hydrological component of the RR should be (i) more accurate than those in the previous R1 and R2, and (ii) rather similar to Noah (except the resolution). The RR also has a higher spatial–temporal resolution than R1 and R2, and covers the time period from 1979 to present.

g. ERA-40 (1957–2002)

ERA-40 (Uppala et al. 2005) is a second-generation global reanalysis, benefiting from the experience of its first-generation 15-yr ECMWF Re-Analysis (ERA-15) and many updates to the ECMWF operational data assimilation system. ERA-40 also has a higher temporal resolution, higher horizontal resolution, and more accurate representation of the atmospheric boundary layer than the older ERA-15. The ERA-40 dataset begins in September 1957 and ends in August 2002 (not kept up to date). The ERA-40 dataset is (until further notice) one of the best global reanalyses and is widely used by the operational and research communities. The horizontal resolution of the ERA-40 used here is 2.5° × 2.5°.

3. Observed and simulated soil moisture variability over Illinois

The seven different land surface datasets described in section 2 were evaluated in multiple manners. Most soil moisture datasets have a common period from January 1984 to December 2003, except for ERA-40 and VIC. When compared with Illinois observations we often employ the ''2-m'' integral (i.e., 2-m column total soil moisture; SM2m), even though some models (i.e., LB and VIC) are not exactly 2 m. A detailed analysis, including profiles, for Illinois observations is given directly below.

a. Annual cycles and interannual variability of observed Illinois SM2m

Although the spatial and temporal resolutions of the observed Illinois soil moisture data are not directly

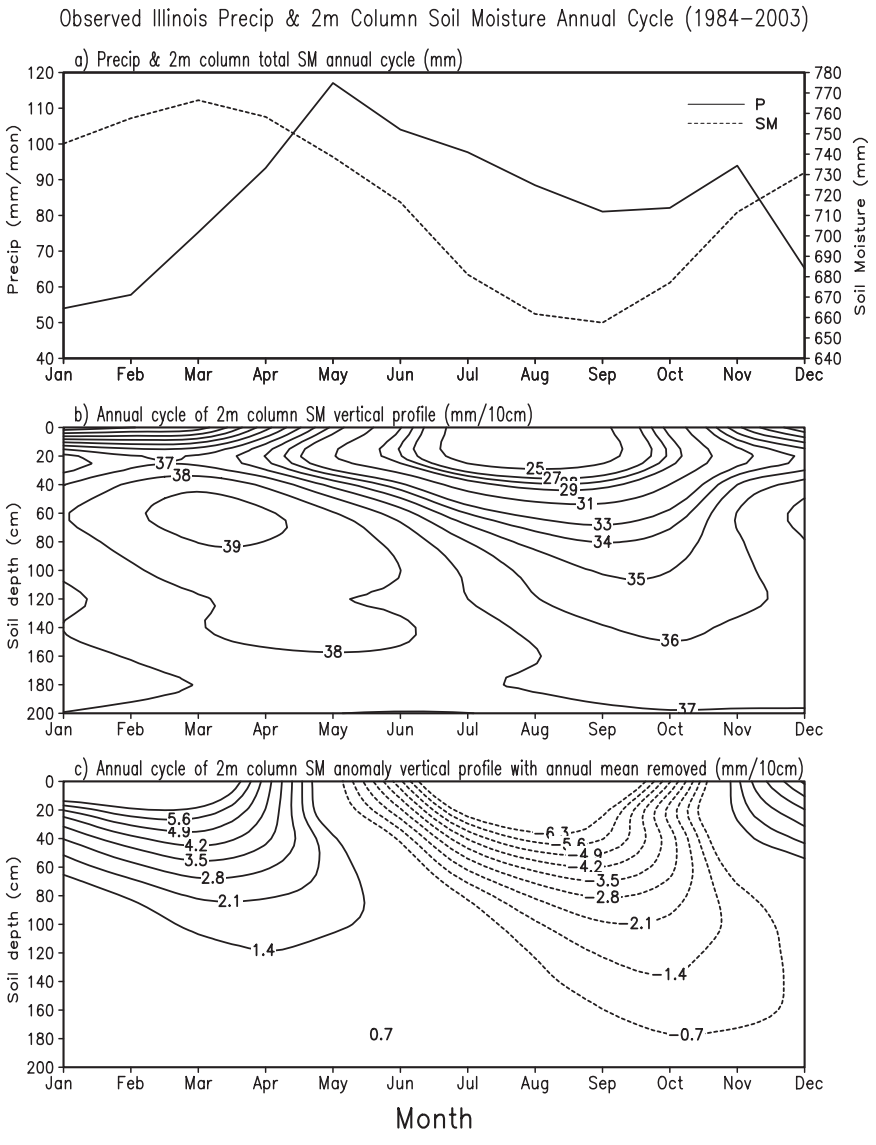

FIG. 1. Annual cycle of observed (a) precipitation and 2-m column soil moisture (mm) and (b) vertical profile 2-m column soil moisture {mm (H_2O) [10 cm (soil)]$^{-1}$} for 1984–2003. (c) As in (b), but with annual mean removed.

compatible with the offline runs and reanalyses, and the (assumed) vegetation covers and soil properties may also be different among the observations and calculated soil moisture datasets, the Illinois soil moisture dataset is the best we have to validate (if not verify) the calculated soil moisture data. In this paper, the data will not be compared station by station. They will be compared only as statewide averages. Also, following Schaake et al. (2004), only 17 sites are used in this study because data from 1 of the 18 sites is quite different from the other 17 sites.

Figure 1 describes the annual cycle of the observed (gridded) precipitation over Illinois and SM2m averaged (station data) from 17 sites over Illinois. Figure 1a shows that although the climatology of the observed precipitation has double peaks (one appears in May and another is in November, i.e., a clear semiannual component), the climatological evolution of SM2m is dominated by an annual cycle mainly, with a maximum (765 mm of water) in March and a minimum (655 mm of water) in September, with an annual range of 110 mm of water. Figures 1b,c present the climatological evolution of the observed soil moisture vertical profile from 11 different soil depths. The soil moisture vertical profile (Fig. 1b) has two maxima. One is in the top layer from January to March and the other is between 50- and 90-cm depths in March and April. The only minimum occurs in August at

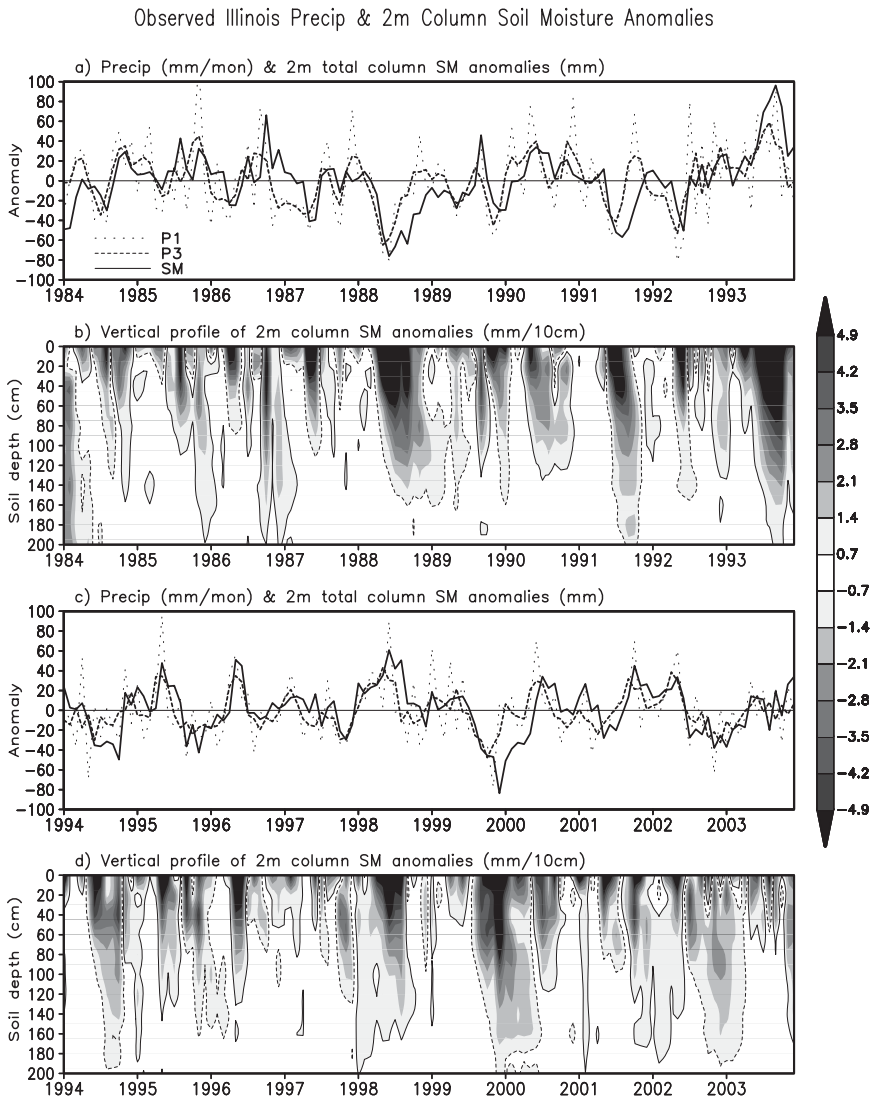

FIG. 2. (a),(c) Observed monthly precipitation (P1), 3-month running mean precipitation (P3), and 2-m column monthly soil moisture anomalies averaged over Illinois (mm). (b),(d) Observed vertical profile of 2-m column soil moisture anomalies [positive (negative) values are inside solid (dashed) contour] is derived from 0–10-, 10–30-, 30–50, 50–70-, 70–90-, 90–110-, 110–130-, 130–150-, 150–170-, 170–190-, and 190–200-cm soil layers {mm (H_2O) [10 cm (soil)]$^{-1}$} for 1984–2003.

0–20-cm depth. A clearer picture emerges when subtracting the annual mean in each layer. Figure 1c shows that the upper soil layer acts like a low-pass filter and under the top layer the annual evolution of soil moisture is much smoother, and its amplitude decreases gradually with depth. The phase shift or delay of the annual harmonic in soil moisture increases with depth and is more than 3 months at the bottom of the 2-m column. This behavior resembles the penetration of the annual cycle in temperature into the soil (Sellers 1965). The results may suggest that to simulate this feature, land surface models need good vertical resolution and physics resembling conduction even for water infiltration.

The interannual variability of observed SM2m and the vertical profile of soil moisture anomalies are given in Fig. 2. The panels (a) and (c) show that the interannual variability of SM2m anomalies largely corresponds to the interannual variability of the precipitation, with some phase delay, as it should be. Another distinguishing feature shown in Figs. 2b,d is that often the variability in the top 40-cm soil layer is noisier. The small events (or anomalies) normally do not percolate to the deeper soil layers. Only larger and more persistent events can

infiltrate, with some delay, to deep soil layers where the amplitudes of soil moisture anomalies can reach values comparable to those of the annual range of climatological mean soil moisture.

b. *Validation of models against observed Illinois soil moisture*

The simulated soil moisture datasets are spatially averaged over all grid points inside a region nominally representing the state of Illinois, bounded by 37°–43°N, 90°–88°W. The number of grid points depends on the model resolutions. The observed results are averaged from 17 stations. Therefore, the readers are advised that all comparisons with the observed soil moisture made in this paper are based on the state average.

1) ANNUAL CYCLES AND INTERANNUAL VARIABILITY OF SIMULATED SOIL MOISTURE

The annual cycle and interannual variability of the observed and simulated monthly SM2m for the period from January 1984 to December 2003 over Illinois are displayed in Fig. 3. The time evolution of both the simulated SM2m anomalies from the Noah NLDAS run and RR (top left panel) follows the observation quite well (correlations with the observations are 0.81 and 0.69, respectively) and most wet and dry events are captured very well. However, both the Noah NLDAS and RR tend to overestimate dry events, such as from 1987 to the early 1990s and after 2000. The annual ranges and phases of the SM2m annual cycles (top right panel) are also well simulated, but with about a one-month delay in the wet peak season and slightly dryer simulated total SM2m than the observation. Overall, the Noah simulated SM2m and annual ranges are closer to the observations than any other models. The annual range in the RR is much (about 2 times) larger than the observation. It is interesting that the Noah and RR simulated soil moisture datasets were generated from a very similar version of the Noah LSM, and forced by the same observed precipitation (although at different spatial resolution) and somewhat different atmospheric forcing fields, with Noah NLDAS from the adjusted R1 output (Fan et al. 2006) and the RR from the NCEP Eta Data Assimilation System (EDAS) (Rogers et al. 2001). Therefore, the soil moisture differences between the Noah NLDAS run and RR, which are larger than we expected, should largely be attributed to the input atmospheric forcing and the difference caused by offline (Noah) versus coupled (RR) calculations. As we will see below the Noah and RR differences are profound.

The time evolution of the SM2m anomalies simulated by the R2 and ERA-40 systems is shown in the (left) middle panel of Fig. 3. The result for R2 is not very good for Illinois; about half the time R2 agrees with the observation but half the time R2 misses the target, while the result from ERA-40 follows the observations better but with too weak amplitudes. Their correlations with the observations are 0.51 and 0.64, respectively. The annual cycles of the simulated SM2m indicate a large dry bias for both R2 and ERA-40. The annual ranges of the simulated SM2m are much smaller than the observations, with ERA-40 showing the least variation. As to the phase of the annual cycle, the R2 is in good agreement with the observation for the wet peak season in late winter while ERA-40 is about one month early. Both R2 and ERA-40 are about one month late for the dry season in September. When comparing with R1, the R1 soil moisture anomalies (not shown) have better agreement (than R2) with the Illinois observations (in that the R1 correlation is 0.57), but over the rest of the CONUS the R2 is better correlated (than R1) with other datasets described in this paper. However, R1's amplitude of annual cycle is much too large (similar to the RR).

The lower panel of Fig. 3 shows the simulated SM2m anomalies and their annual cycles from LB and VIC. The simulated soil moisture anomalies from both runs reproduce the observed anomalies fairly well (correlations with the observations are 0.74 and 0.84, respectively), with the LB tending to slightly overestimate the dry events. The annual ranges of total column soil moisture from the two runs are comparable with the observations, but much drier in the annual means (it is not a completely fair comparison, considering that the depth of the leaky bucket model is 1.6 m and the VIC LSM has a varying depth from 1 to 2.3 m, while the depth of the observed soil moisture is 2 m; Fig. 15 will further address this issue). The phases of the simulated soil moisture annual cycles in LB and VIC agree perfectly with the observations for the dry season, but with a one-month delay for the peak of the wet season.

2) ANNUAL EVOLUTION OF TOTAL COLUMN SOIL MOISTURE STANDARD DEVIATION

The annual cycles of the observed and simulated standard deviations of monthly SM2m over Illinois for 1984–99 are depicted in Fig. 4. The standard deviation is defined as

$$\mathrm{Std}(m) = \sqrt{\frac{1}{n}\sum_{i=1}^{n}(X_{i,m} - \overline{X_m})^2},$$

where variable $\overline{X}$ is the climatology of X, m is month of the year, i is the year, and n is total number of years. The

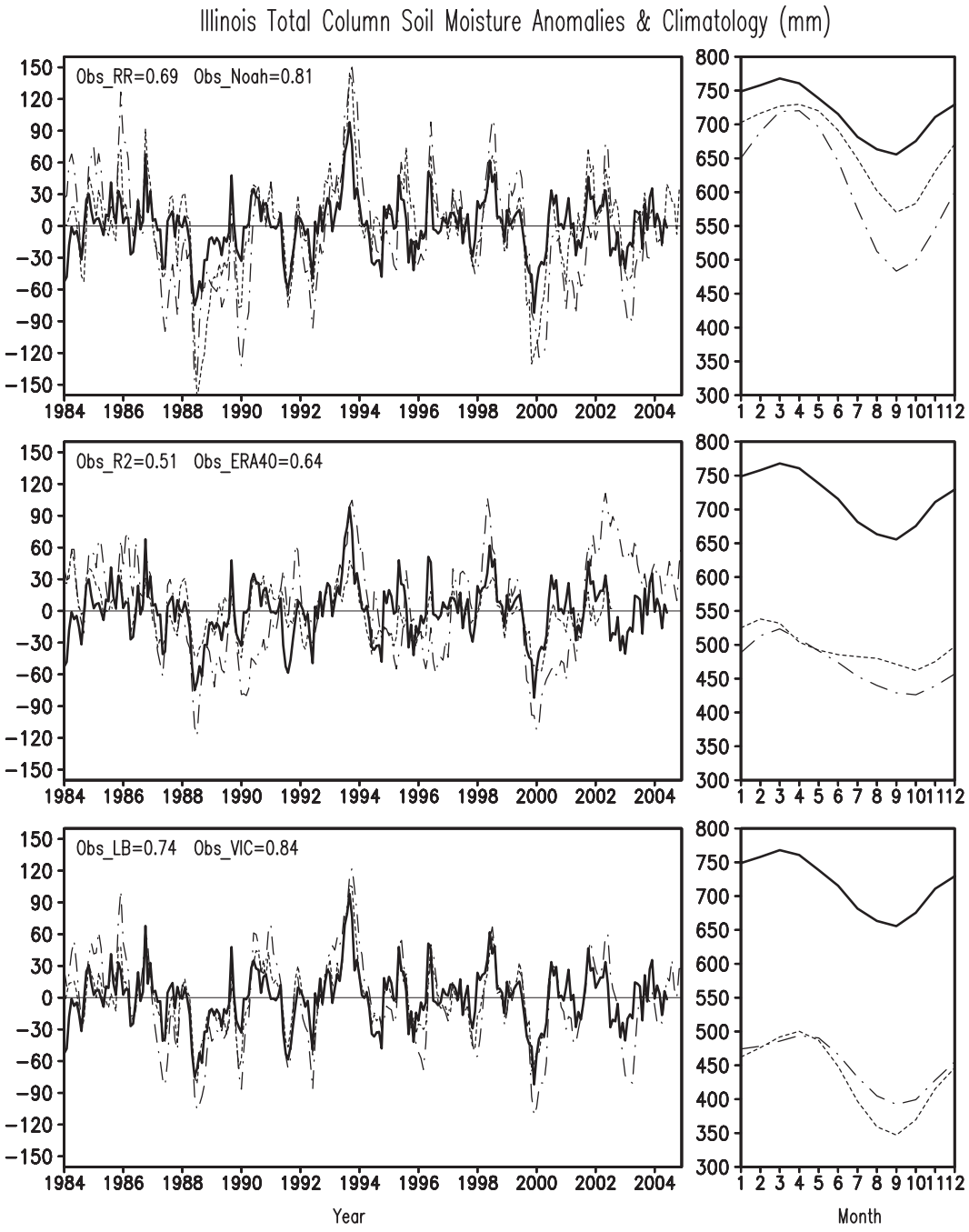

FIG. 3. The (left) monthly anomalies and (right) mean annual cycle (averaged for 1984–99) of the observed (solid) and simulated 2-m column soil moisture (dashed = Noah, ERA-40, VIC; dotted–dashed = RR, GR-2, LB) in the Illinois area for 1984–2004 (mm). The numerical values are the anomaly correlations between the observed and simulated soil moisture anomalies for six models for 1984–99.

observation reveals that the soil moisture has the smallest variability in the spring season (when soil moisture in Illinois tends to peak climatologically) and the largest variability in the warm season, including September. A large spread was found in the simulated SM2m's standard deviation. Most models have too high standard deviation, except VIC and ERA-40. One model (ERA-40) completely lacks an annual cycle in standard deviation, while all others have a maximum at some point during the warm season and a minimum at some point in spring.

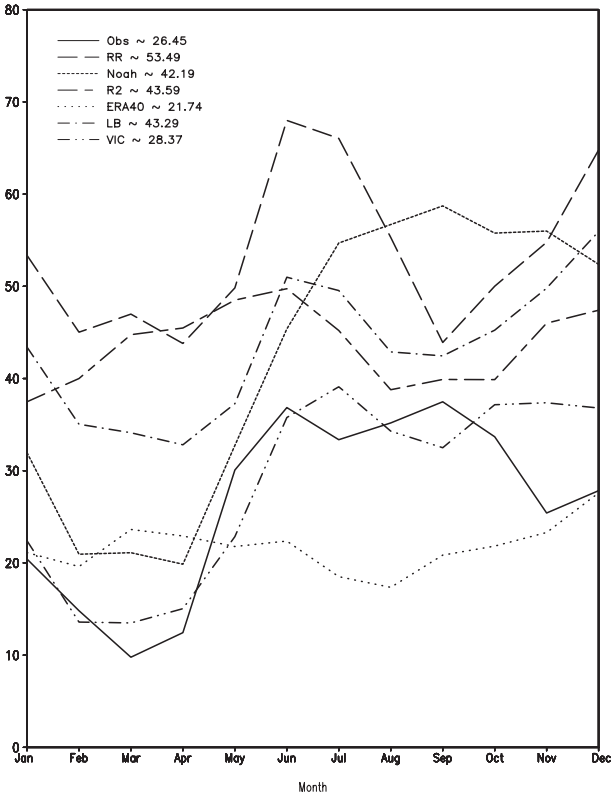

FIG. 4. Annual cycle of the standard deviation for observed and simulated 2-m column soil moisture anomalies in Illinois for 1984–99 (mm). Values in the inset are annual means.

The standard deviation from the Noah NLDAS agrees fairly well with the observation in the spring season, but is too large in other seasons (especially in the warm season), which is consistent with its overestimation of dry events noted earlier. In general, the RR has the largest standard deviation of all and its annual evolution is consistent with the RR tending to overestimate the soil moisture anomalies in both wet and dry directions, but especially so for the dry events in the warm season. The results from R2 and LB have features similar to those of RR but with smaller errors, while ERA-40 is flat throughout the season. An offline run (Van den Hurk et al. 2008), made with the same land surface scheme used in ERA-40, also showed similar flat features of soil moisture standard deviation in several different places in Europe. Among all simulated soil moisture datasets used in this study, the annual cycle of simulated soil moisture standard deviation from the VIC NLDAS run has the best agreement with the Illinois observation in most seasons, except November and December.

It should be noticed that the comparison here is not completely fair, considering that some land surface models have different layers and depths.

3) WAVELET ANALYSIS FOR ILLINOIS SM2M ANOMALIES

Wavelet analysis (Torrence and Compo 1998) was used to explore and compare the evolution of observed and simulated soil moisture anomalies in the time and frequency domain. The first 3 yr (i.e., 1981–83 were quite different from the data in the other years because of a change in the instruments) of the Illinois observed soil moisture data were "repaired" by removing the 3-yr annual mean and then replacing it by the annual mean for 1984–2003. The main purpose here is to investigate to what extent the simulated soil moisture anomalies can catch the evolution features of the observed soil moisture anomalies in different time–frequency bands. The local wavelet power spectrum of observed and simulated soil moisture anomalies is presented in Fig. 5. Here the focus is on the area above the "ship hull" to avoid the edge impacts. The observed soil moisture anomalies show that there was large power at 12–18 months, and 3–5-yr periods from the mid-1980s to the mid-1990s. The results from the VIC NLDAS, LB, Noah NLDAS, and ERA-40 almost perfectly reproduce observed features. The observed main features and even some details are well captured by the four models. The performance of RR is slightly worse but it too simulates some of the observed wavelet structures. The performance of R2 (not shown) is discouraging and has too much power in lower-frequency bands.

4) ANNUAL CYCLES AND INTERANNUAL VARIABILITY OF ALL WATER BUDGET COMPONENTS

The evolution of land surface water (or soil moisture) is determined by how the incoming precipitation is balanced by evaporation and runoff. The land surface water budget equation can be written as

$$dw/dt = P - E - R,$$

which depicts the balance between surface water storage change dw/dt (w represents total soil moisture, which for some models includes snowpack and canopy water) and $P - E - R$, which includes total precipitation (P), total evaporation (E; from all sources, some models may have more terms, viz., evaporation of canopy interception, transpiration, evaporation from top soil surface, and sublimation from snowpack), and total runoff (R; surface runoff + subsurface runoff; some models have loss to groundwater). The dw/dt is evaluated with a one-month time step, for example, end of April minus end of March.

Figure 6 shows annual cycles of all land surface water budget components averaged over Illinois. Since no observed evaporation and runoff were available, only

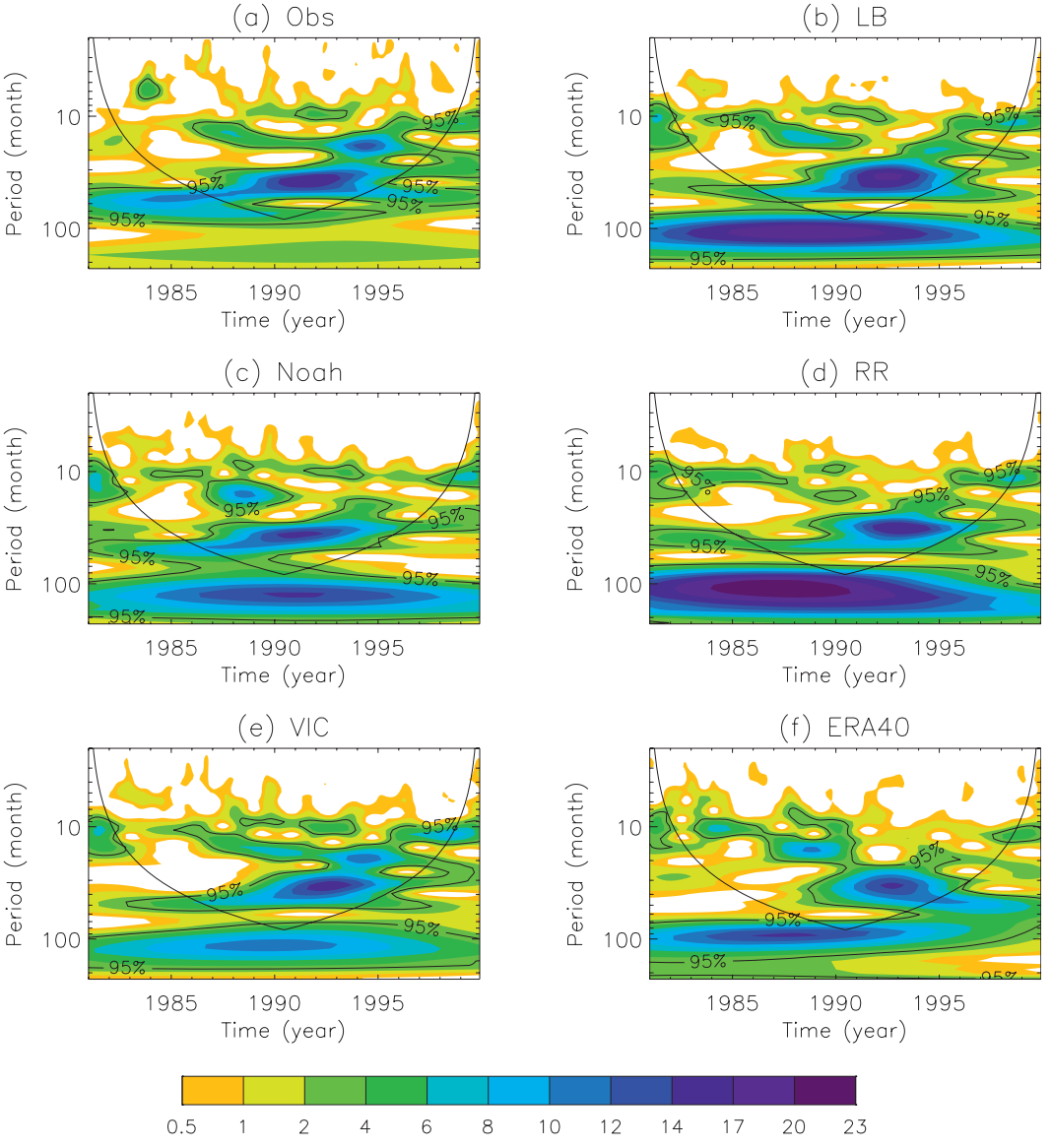

FIG. 5. Wavelet power spectra of total column soil moisture anomalies for 1981–99 over Illinois from (a) observations, (b) LB, (c) Noah, (d) RR, (e) VIC, and (f) ERA-40, normalized by their own squared standard deviations, respectively. All values are greater than zero and less than 23. The areas above the 95% significance level of red noise are marked and contoured with black lines. The ship's hull is the line of demarcation, and anything below the line is dubious because of edge effect and insufficient record length for longer periods.

the six modeled results are given here. Because the three offline runs (Noah, VIC, LB) as well as RR used the observed precipitation as input, the P looks almost identical in those four plots. ERA-40 and R2 used the model-generated precipitation and their annual cycles are noticeably different from the observations, with ERA-40 having lower precipitation in the spring and fall. It should be noticed that during the interactive run, R2 first used model-generated precipitation to force the land surface model and then used observed precipitation to do a "bias correction" 5 days later (i.e., added the difference between observed and modeled rainfall during a 5-day period with opposite sign to the next 5 days). For the simulated evaporation, the annual cycles from Noah, VIC, and ERA-40 look very similar and are comparable, while RR has the strongest evaporation in Illinois in the warm season by far and R2 has the second highest E. The LB (tuned for runoff in Oklahoma) has the weakest evaporation of all six models and shuts down the evaporation in the winter season much more so than other models.

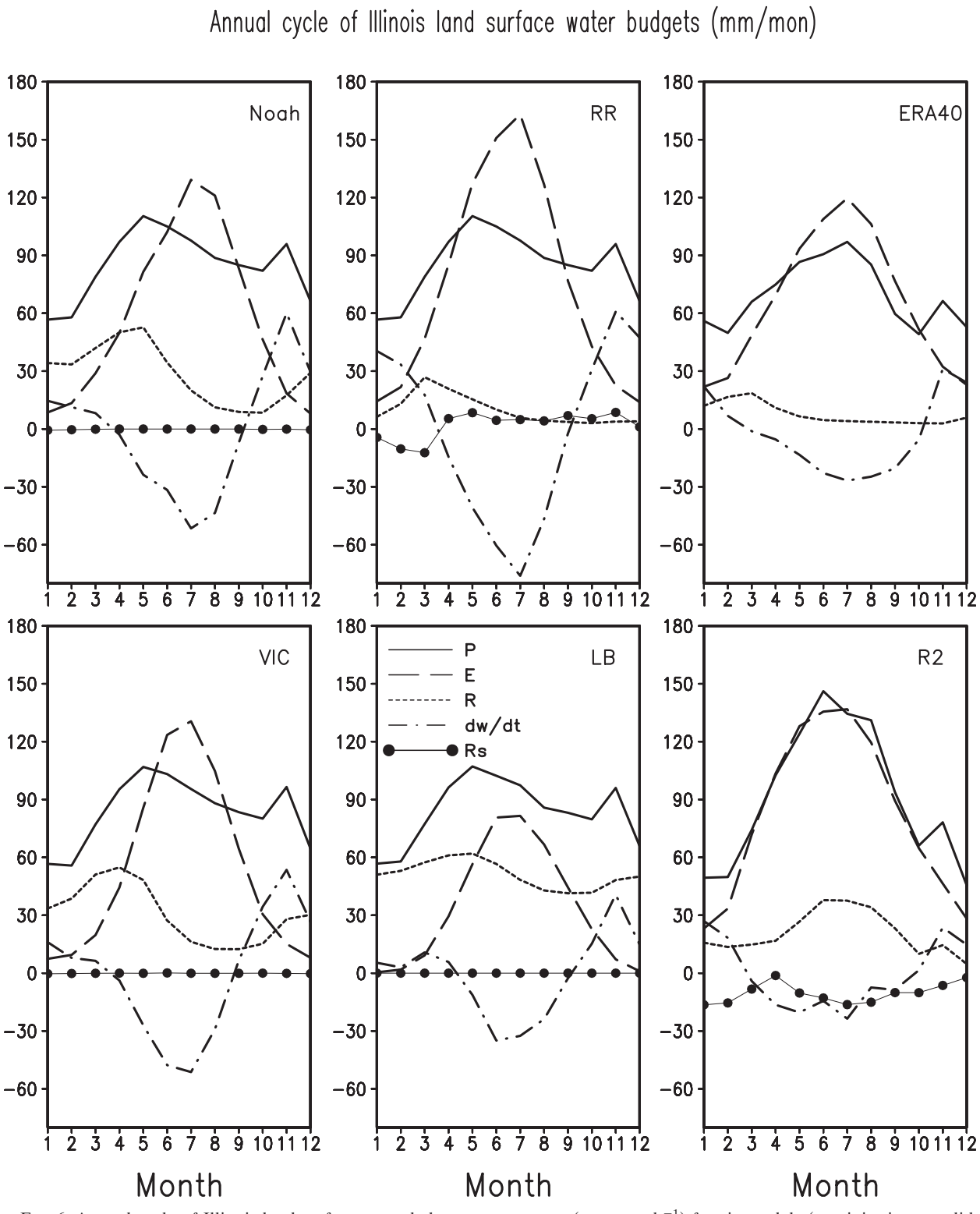

FIG. 6. Annual cycle of Illinois land surface water balance components (mm month^{-1}) for six models (precipitation = solid line; evaporation = dashed line; runoff = dotted line; *dw*/*dt* = dashed–dotted line; and residual = solid line with closed circle for 1984–99).

For the annual cycles of simulated runoff, both the Noah and VIC NLDAS runs have very similar amplitude and phase variations. The runoffs in the three reanalyses are very small in general and stronger in LB in all months except during springtime. The old dichotomy between models that evaporate (meteorology) or run off (hydrology) (Chen et al. 1997, their Fig. 10) is still very visible. Even modern reanalyses (ERA-40, RR) have little or no runoff—a strange error.

As to the annual cycles of total surface water storage change (dw/dt), all models present a similar feature in Fig. 6: land surface water has net depletion in the warm season and is recharged in the cold season. Again, the annual cycles of (dw/dt) from the Noah and VIC runs have very similar amplitude and phase variations. So their climatological soil moisture variations should have a similar annual range as well (see Fig. 3). The RR has the largest (dw/dt), caused by its presumably excessive evaporation in the warm season. Therefore, RR has the largest annual ranges of soil moisture (Fig. 3). The annual cycle of (dw/dt) from ERA-40 was not directly available and it was estimated as the residual of $P - E - R$. The annual cycles of (dw/dt) from both ERA-40 and R2 are much weaker than other models. Therefore, their annual ranges of soil moisture (integral of dw/dt) are relatively small (see right panels in Fig. 3).

Because the annual cycle of soil moisture is determined by the integration of (dw/dt), and (dw/dt) largely corresponds to the annual cycle in E, the climatological annual cycle in soil moisture (w) is mainly a response to the E forcing, which is very high (low) in summer (winter), with w lagging the extremes of E. This may be why soil moisture has a simple, large annual cycle, even when P does not (cf. Fig. 1).

Finally, Fig. 6 shows that the land surface water budget components in the three offline runs are well balanced. A budget problem has been seen in the reanalyses (see also Roads et al. 2003), especially in the cold season, indicating there were still some difficulties in conserving water in the processes of cold season physics. All models present the picture that evaporation is the most important if not dominant factor to balance incoming precipitation in the warm season. The single exception is the LB where the runoff plays an important role, even in the warm season. The three offline runs indicate that runoff is dominant in balancing incoming precipitation in winter, while the three reanalyses show that the evaporation and runoff both play a role in winter.

The interannual variability of the 3-month running mean of all water budget components over Illinois is given in Fig. 7 (for clarity we only display part of the common period, i.e., 1984–99). The observed P interannual variations (upper panel) from the three offline runs and RR closely follow one other, as they should. Overall, the P interannual variability in ERA-40 is better than that in R2 (however, both badly missed the positive anomalies in 2000; not shown). For the simulated interannual E variations, one of the most distinguishing features is the relatively small amplitude all the time when compared to the amplitudes of their annual cycle or to the interannual rainfall anomalies, except in one particular year (1988) for a few of the models. For the simulated interannual R variations, their amplitudes are relatively larger than those of E but not as high as P. The three offline runs normally follow one another very well. The R variations of RR and ERA-40 are very small most of the time and the results from R2 are sometimes out of phase with the others. Among all land surface water budget components, the simulated interannual variations of (dw/dt) agree best with one another.

Figure 7 also shows that the interannual variations of both R and (dw/dt) correspond to the interannual variations of P. Both of them follow (or correlate positively with) the interannual variations of P fairly well. The above results thus indicate that the interannual variations of P are mainly balanced by the interannual variations of R and (dw/dt), and E anomalies are of secondary importance.

The results in this section have displayed clearly that among all land surface water budget components, E has the most prominent annual cycle, but its interannual variability is very small, except in 1988 for some models. For the other components (i.e., dw/dt, P, and R), the amplitudes of both their annual cycles and interannual variations are comparable. In general, this is also true in other places over the CONUS.

It is interesting (Fig. 7) that (dw/dt) (lhs term of the water budget equation) has more agreement (or correlates highly) among all land surface datasets used here [the (dw/dt) correlations among the Noah, VIC, LB, and RR range from 0.88 to 0.95, ERA-40 with others are from 0.83 to 0.86, and R2 from 0.64 to 0.76]. Even though we may not know E and R on the rhs of the water budget equation very well, apparently $E + R$ is very similar among models.

Section 3 was about verification against observations and thus focused on Illinois. The rest of the paper is an intercomparison for the entire United States but has no strict verification.

4. Spatial–temporal features of simulated land surface datasets over the United States

Since long-term and consistent in situ soil moisture observations over the CONUS are not available, here an intercomparison of six (three offline runs and three

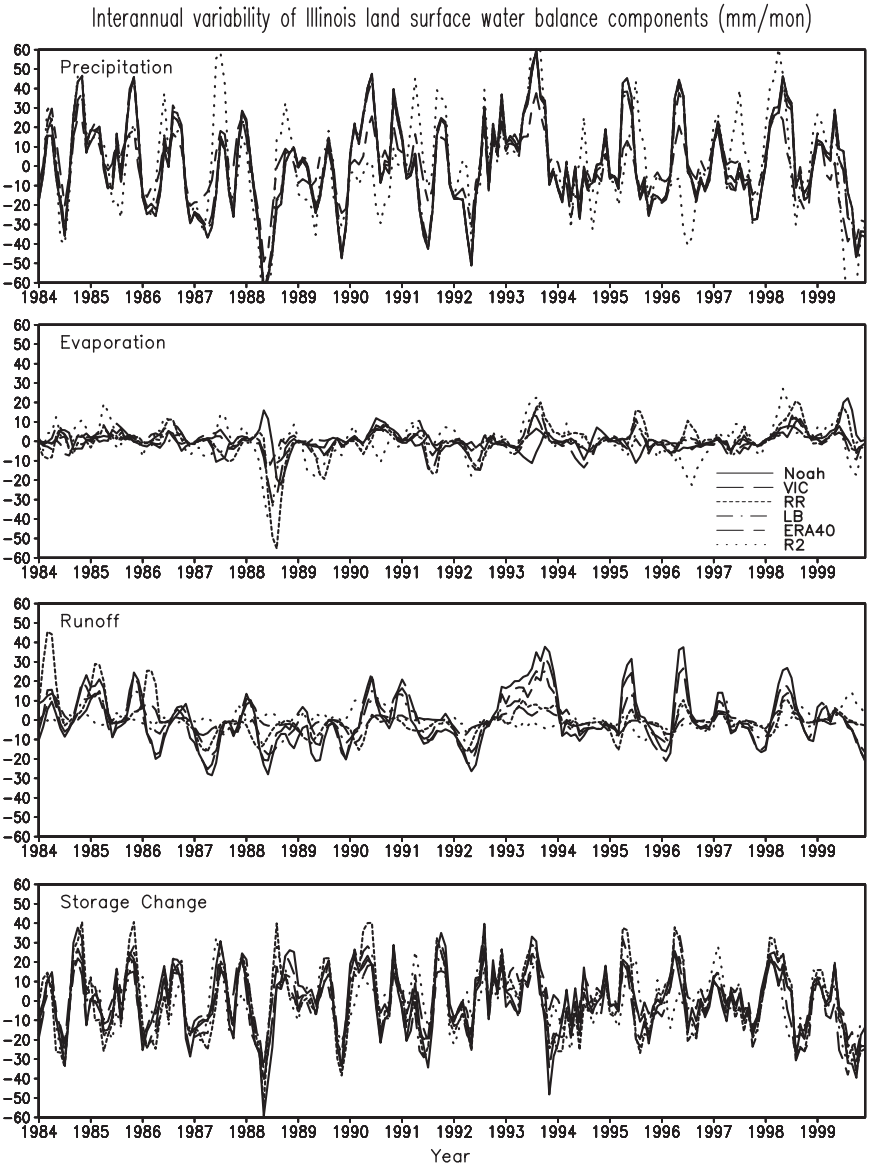

FIG. 7. Interannual variability of Illinois land surface water balance components (mm month^{-1}) for six models for 1984–99 (P, E, R, and dw/dt from top to bottom). Precipitation is observed (except GR-2 and ERA-40); other variables are calculated.

reanalyses) simulated soil moisture datasets is conducted to gain some impressions about their basic statistical features, including spatial–temporal evolution.

a. Annual mean standard deviation (MStd) of simulated total column soil moisture

The spatial distribution of the annually averaged standard deviation [i.e., $\mathrm{MStd} = \{(1/12)\sum_{m=1}^{12}[\mathrm{Std}(m)]^2\}^{1/2}$; see standard deviation equation for definition of Std(m)] from six simulated soil moisture datasets over the CONUS for the period of 1980–99 is shown in Fig. 8. A common scale is used to facilitate comparison. A map aggregated value is given in the lower right corner. Apart from resolution, remarkable differences are found among different datasets as already noted for Illinois (Fig. 4). In general, RR and R2 have the largest soil moisture variability over the United States. For Noah and LB, large soil moisture variability is mainly located in a band from south to north in the central CONUS. For VIC, large soil moisture variability appears in the northwest CONUS in fine-grained fashion. ERA-40 has the weakest soil moisture variability over the CONUS, and does not even have much spatial

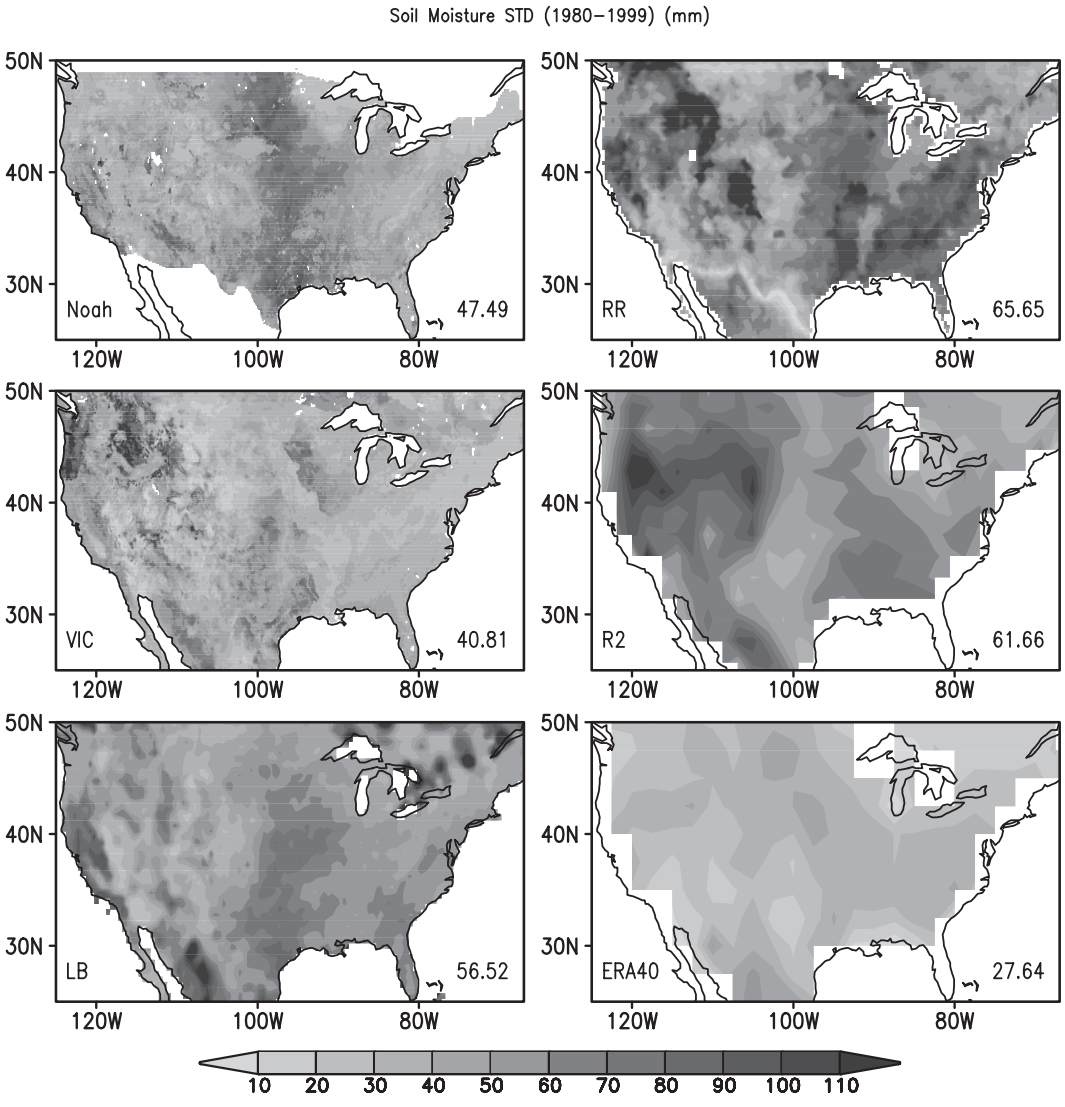

FIG. 8. Annual mean soil moisture standard deviation (mm) over CONUS (1980–99) for six models. All maps have the same scale. The number in the lower right corner is the mean over CONUS.

structure. However, the Noah, VIC, LB, and RR, which are all forced with observed precipitation, do show some common features, such as relatively large soil moisture variability somewhere from south to north in the central United States. It is interesting that the large soil moisture variability over the central United States is located over the transition region from dry to wet climate, which is one of the so-called hot spot areas (Koster et al. 2004), as well as over the western fringe of the area with the largest standard deviation in the observed precipitation (Huang et al. 1996; see also Fig. 10). The large differences between Noah and RR runs suggest that the offline versus interactive (or different atmospheric forcing) aspects play a very important role in soil moisture variability.

b. Annual mean standard deviation of water budget components (dw/dt, P, E, and R)

The next four figures (Figs. 9–12) show spatial patterns of MStd for dw/dt, P, E, and R, respectively, over the CONUS for the period of 1980–99. Unlike the standard deviation of the simulated soil moisture (Fig. 8), the variability of (dw/dt) in Fig. 9 does display more common features among different datasets, especially for the three offline runs and RR. For the three offline runs and RR, the spatial pattern of MStd of (dw/dt) bears resemblance to a spatial pattern of observed precipitation standard deviation (Fig. 10). The main differences among models are in the western U.S. mountain region, where the Noah

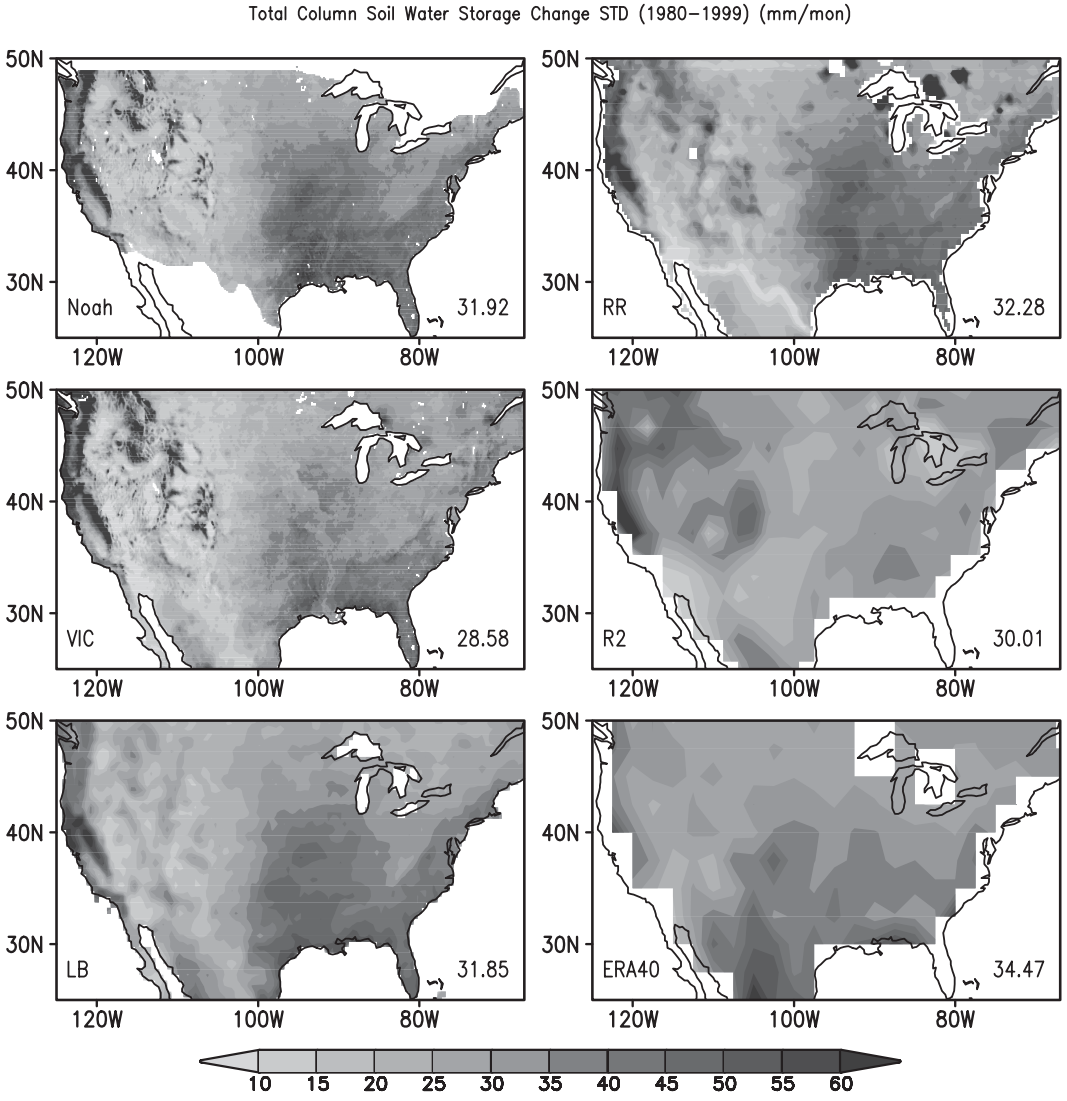

FIG. 9. Annual mean standard deviation of total column water storage change (dw/dt; mm month^{-1}) over CONUS for 1980–99. The number in the lower right corner is the mean over CONUS. All maps have the same scale.

and VIC runs and RR used the Parameter-elevation Regressions on Independent Slopes Model (PRISM; Daly et al. 1994) adjusted precipitation, while the LB used observed precipitation without the PRISM adjustment. The RR precipitation [also see signature in w (Fig. 8), dw/dt (Fig. 9), and E (Fig. 11)] MStd presents lower values along the United States–Mexico border, which is caused by a problem in its precipitation mask. ERA-40 precipitation has a strange pattern. For the spatial pattern of MStd of P (Fig. 10), all models agree well, except ERA-40.

For MStd of E (Fig. 11), its amplitude is about ⅓ of MStd of dw/dt and P (note different scales used), and also has very different spatial distributions among different datasets. For the MStd of R (Fig. 12), it seems the major variances are located along the western U.S. coast and mountain regions, and in some models, in the southeastern United States. The Noah and VIC runs have very similar amplitudes and spatial patterns. The LB, RR, and R2 have similar spatial patterns to the above two NLDAS runs, but different amplitudes. The MStd of R from ERA-40 is small and quite different from others.

The very similar patterns among three offline runs and RR (Figs. 9, 10) suggest that the other atmospheric forcing and model differences may play a limited role in the interannual variations of (dw/dt); that is, the interannual variability of precipitation forcing is the most dominant factor in determining the interannual variability of (dw/dt) and thus (by integration) w. This is consistent with the results for Illinois from Fig. 7, where

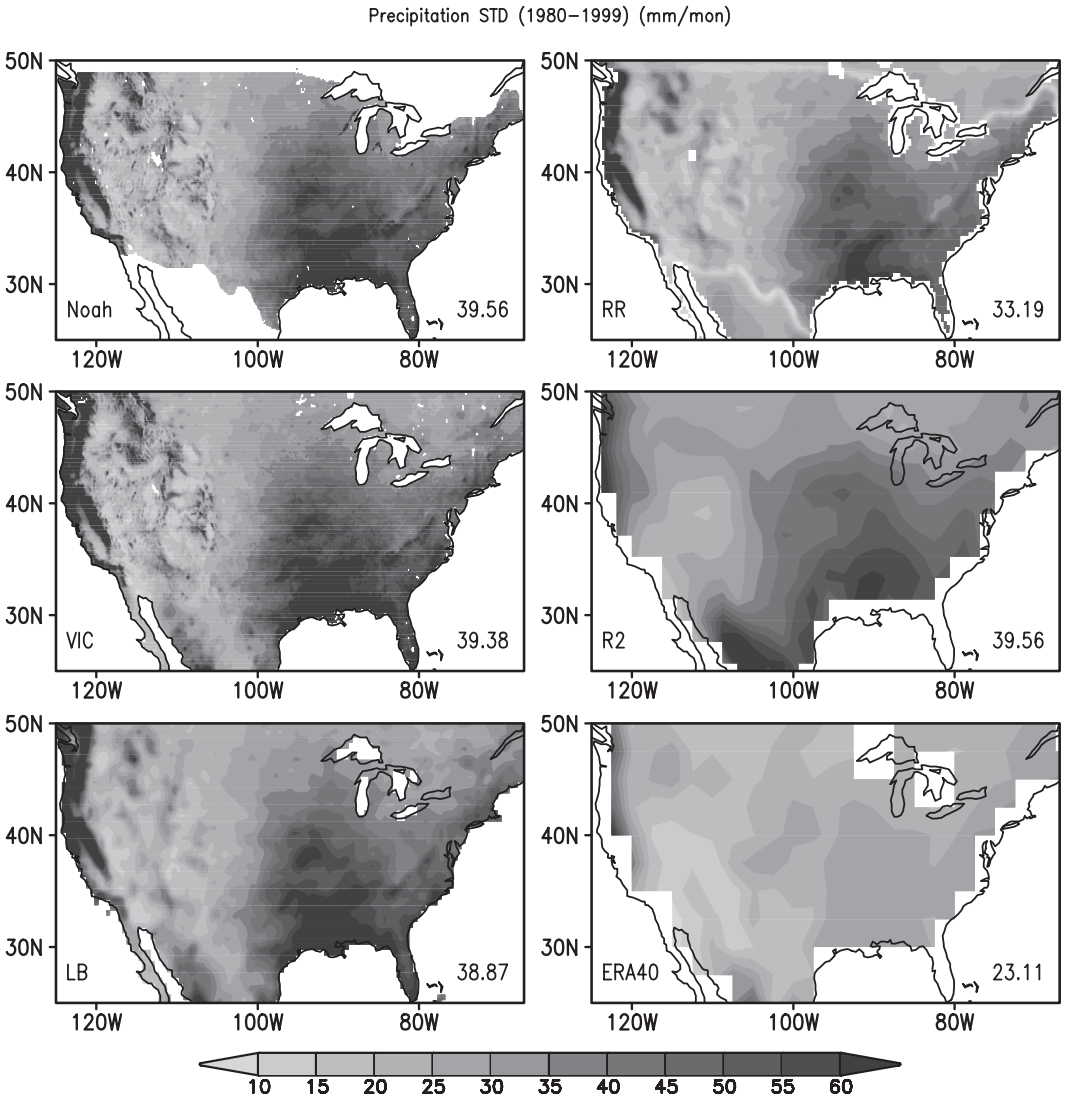

FIG. 10. As in Fig. 9, but for precipitation.

the interannual variations of precipitation were found to be highly correlated to the interannual variation of (dw/dt) (0.86, 0.87, 0.88, 0.93, 0.93, and 0.79 for Noah, VIC, RR, LB, ERA-40, and R2, respectively). This is different from the annual cycle of (dw/dt) (Fig. 6), which is determined by the partition of the P annual cycle into E and R annual cycles. The MStd of (dw/dt) from R2 and ERA-40 (Fig. 9) shows different patterns that should be caused by the difference in their precipitation inputs.

c. *Spatial–temporal correlation of total column soil moisture anomalies*

It is interesting to know how well the simulated soil moisture datasets spatially–temporally resemble one another in terms of anomalies. The anomaly correlation is defined as

$$\rho(s) = \frac{\sum_s X(s)Y(s)}{\left[\sum_s X^2(s)\sum_s Y^2(s)\right]^{1/2}},$$

where X and Y are two anomaly variables, s is either time or space points (or both), and the summation is over s.

Figure 13 depicts the temporal correlations among different simulated soil moisture anomalies over the CONUS for all months in 1980–99. The most notable features are that the simulated soil moisture anomalies from the three (Noah, VIC, and LB) offline runs are very well correlated in time over almost the entire CONUS.

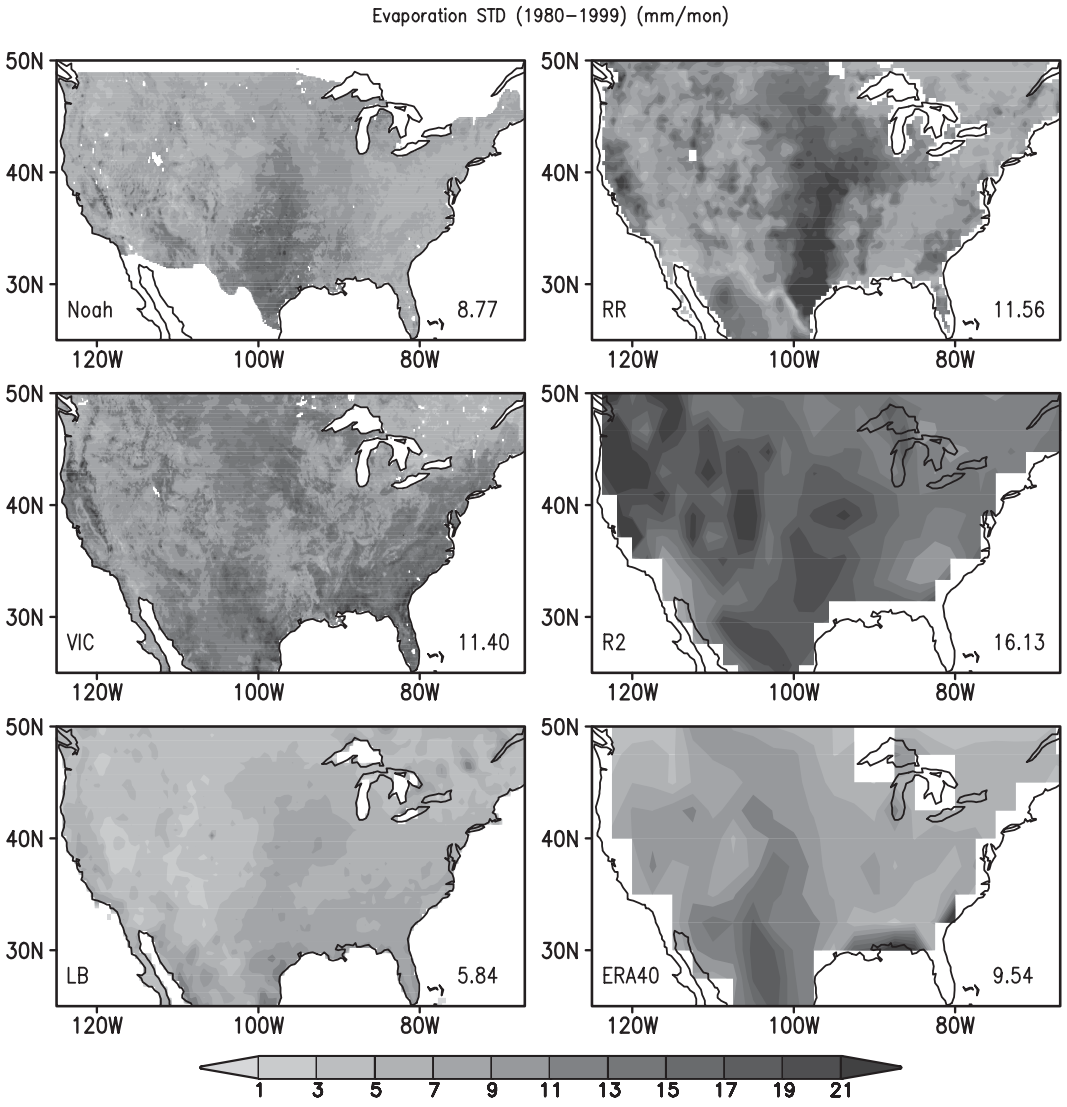

FIG. 11. As in Fig. 9, but for evaporation (note much reduced scale).

The next best correlated model is RR, with some degradation in the Midwest and Northeast. The fifth one is ERA-40, with a further decrease in correlation mainly from New Mexico to Montana and in the central-east CONUS for most models but still fairly well correlated with other parts in the rest of the CONUS. On average, R2 has the lowest correlation with the other soil moisture datasets. It seems that the hardest place (simulated soil moisture anomalies did not agree between any two models) is around Utah and Colorado and the best place is the southwest and the central United States (even though the mean and the standard deviation among models disagree). The CONUS-wide averages (over all grid points) are given in the upper right corner in Table 1. The results in this table reinforce the conclusion that the offline models are much more highly correlated to each other than the interactive models.

The time evolution of spatial pattern correlations of soil moisture anomalies between any two models over the CONUS for the period of 1980–99 is shown in Fig. 14. Although highly positive in general, noticeable variations in the correlations can be seen for all paired datasets. For those times when the spatial correlations were quite low (i.e., May 1982), the patterns of simulated soil moisture anomalies are loosely organized and more small scale and low amplitude. When the spatial correlations are high (i.e., July 1989), the patterns of simulated soil moisture anomalies tend to be more large scale and high amplitude (not shown). Similar to the temporal correlations, on average the spatial patterns of the simulated

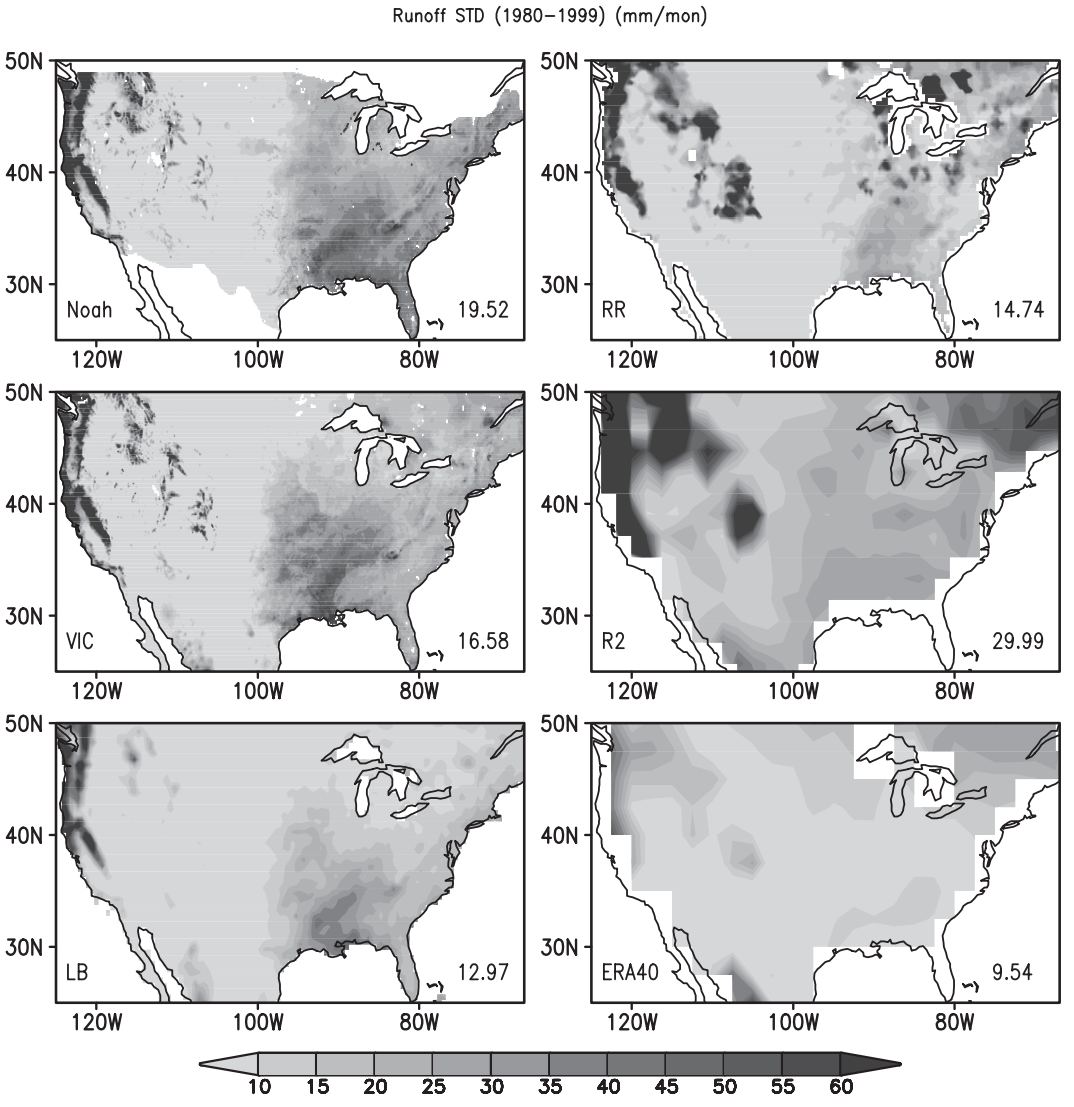

FIG. 12. As in Fig. 9, but for runoff. The number in the lower right corner is the mean over CONUS.

soil moisture anomalies from three offline runs are fairly well correlated and are among the most similar. The next one is RR followed by ERA-40. R2 has the lowest spatial correlations with the other soil moisture datasets nearly all the time. It is interesting that LB tends to be closer (or highly correlated) to others (i.e., Noah, VIC, and RR; see solid lines in Fig. 14). The averaged (over all months of 1980–99) spatial correlations, along with temporal correlations, over the CONUS are given in the lower left corner in Table 1.

d. Simulated hydrological extreme events: 1988 drought and 1993 flood

Land surface hydrological extremes, such as droughts and floods, have major impacts on life, property, and economic activities. The large-scale and widespread 1988 drought and 1993 flood in the United States are main examples. Both of them were among the worst and most costly natural disasters in U.S. history and damages caused by each of them exceeded $40 billion and $20 billion, respectively (http://lwf.ncdc.noaa.gov/oa/reports/billionz.html). Two of the more interesting questions are whether the land surface simulation systems can capture these worst droughts and floods properly and how they distribute in space? Since the mean and variability of different soil moisture datasets are quite different, standardized soil moisture anomalies were used here to make a relatively fair comparison (Koster et al. 2009). The simulated 1988 summer drought and 1993 summer flood from six land surface datasets are presented in Figs. 15a,b,

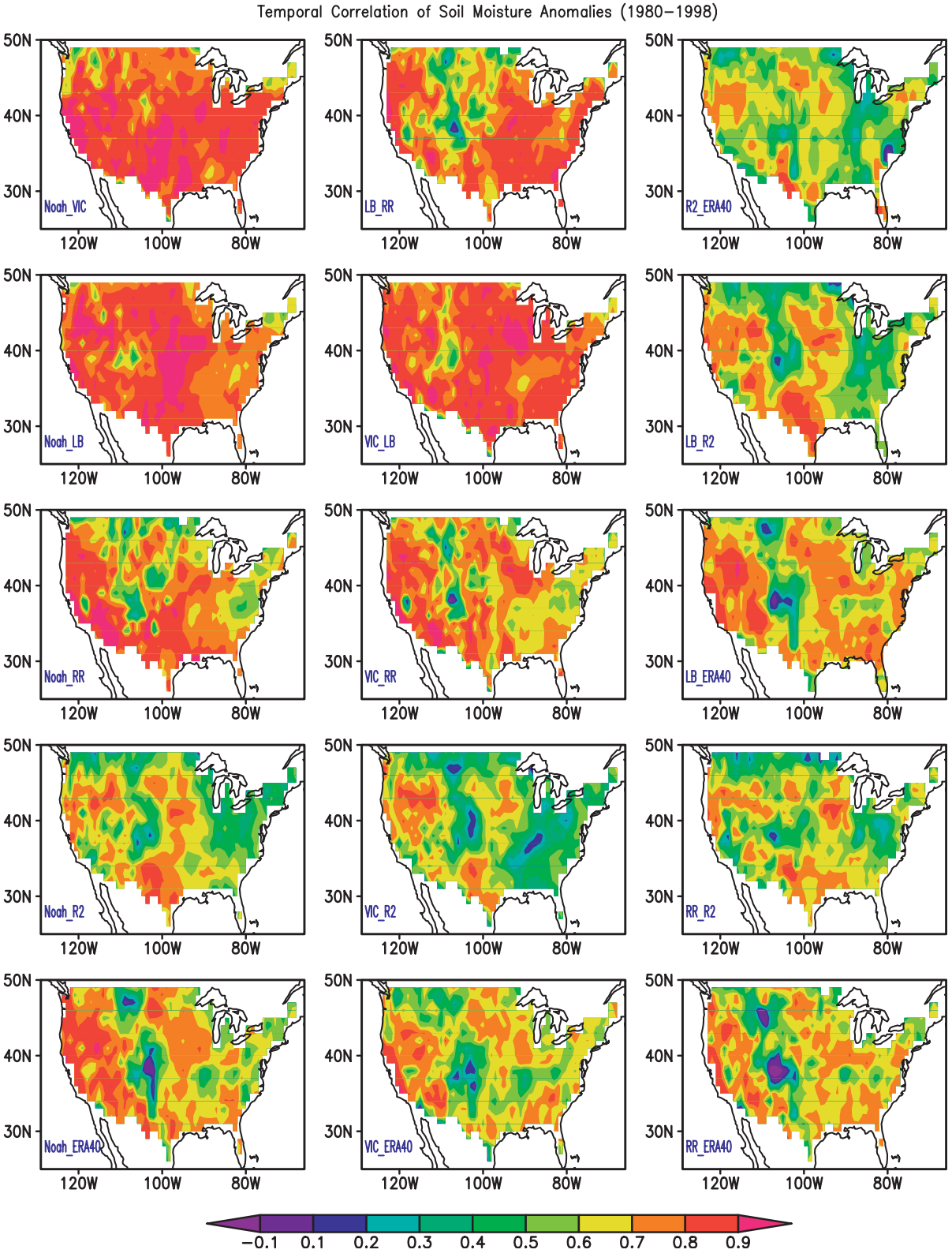

FIG. 13. Temporal correlation among different soil moisture anomaly datasets over CONUS for all months for 1980–99. The letters (i.e., Noah_LB) in the lower left corner refer to the correlations between the two (Noah and LB) datasets.

TABLE 1. Correlation of soil moisture for seven models over the United States. The temporal anomaly correlations for the period of 1980–99 averaged over the United States are shown in the upper right half of the table. Spatial anomaly correlations over the United States averaged for the period of 1980–99 are shown in italics in the lower left half of the table. Values above 0.6 are in bold.

Spatial	Noah	VIC	LB	RR	R2	R1	ERA-40	Temporal
		0.80	**0.79**	**0.70**	0.58	0.49	**0.65**	Noah
VIC	***0.67***		**0.80**	**0.70**	0.53	0.39	**0.62**	VIC
LB	***0.76***	***0.74***		**0.73**	0.60	0.41	**0.67**	LB
RR	*0.58*	***0.60***	***0.68***		0.58	0.32	**0.61**	RR
R2	*0.45*	*0.44*	*0.50*	*0.47*		0.46	0.57	R2
R1	*0.41*	*0.35*	*0.40*	*0.31*	*0.39*		0.43	R1
ERA-40	*0.55*	*0.48*	*0.56*	*0.49*	*0.47*	*0.41*		

respectively. The major features of the 1988 summer drought over a large part of the CONUS are well captured by all six land surface datasets, with large negative soil moisture anomalies from northwest, central-northwest to central-southeast. However, some noticeable differences are also observed, such as the degree of drought severity and the locations affected. Overall, the simulated 1988 summer drought from the VIC NLDAS run was relatively weaker (in terms of standardized departure from its own mean) and more spotty (in terms of severity) than the others.

For the simulated 1993 summer flood, the extremely large positive soil moisture anomalies in the upper Mississippi and Missouri River basins and dry condition to the east were well simulated by almost all six land surface datasets. The moderate drought in the southeast CONUS was also well captured, except by R2. The three offline runs and RR have very similar spatial anomaly patterns. R2 missed the drought condition in the southeast CONUS. Another feature is that the Noah and VIC runs with $\frac{1}{8}^\circ$ high spatial resolutions give more detailed spatial structures of the severity of drought and flood.

5. Summary and discussion

A long-term, accurate, homogeneous land surface dataset that can be routinely updated is crucial for monitoring land surface conditions in the past and real time; understanding land surface processes; evaluating, developing, and improving land surface models; and eventually for improving our understanding and prediction of weather and climate variations. In this study, the observed soil moisture data over Illinois and six simulated multidecade land surface datasets were used to evaluate and explore the spatial–temporal features of observed and simulated land surface hydrological variations over the CONUS.

The amplitude of the annual cycle of the observed soil moisture vertical profile over Illinois decreases with depth, while its phase shift increases with depth. Soil moisture variations at 2-m depth are very small. Both the annual cycle and interannual variability of the observed soil moisture vertical profile show that the top-50-cm soil layer acts like a low-pass filter and small and fast events tend not to infiltrate to deeper soil layers. Observed interannual soil moisture variations are largely driven by low-frequency variations in precipitation. These results may give some hints of how to upgrade land surface models. For example, a previous study (see Fig. 6 of Fan et al. 2006) indicated that the simulated soil moisture anomalies from the Noah LSM showed notably less vertical gradient than the observations. The most likely cause is the uniform profile of root density applied in the Noah LSM. This suggests that the LSM may need more layers, especially in the top-1-m soil column.

The simulated annual cycle and interannual variability of total column soil moisture from all models reasonably follow the observed soil moisture variations in Illinois. In general, in terms of temporal anomaly correlations the offline runs are closer to observation than the reanalyses. For the seasonal variation of the standard deviation, only the VIC NLDAS offline run more closely follows the observation most of time—the variations of standard deviation from the Noah NLDAS run, LB, RR, and R2 are much too large, while the variation is small and without clear seasonality in ERA-40. Wavelet analysis shows that most of the simulated soil moisture can reasonably well capture the observed soil moisture variability in time-frequency domain, with the VIC, Noah, and LB offline runs among the best, while R2 is an outlier when compared with other models.

The analysis of water budget components presents the basic features of annual cycles of each component and offers possible explanations for features of the soil moisture annual cycle. Interannual variability of water balance components shows that anomalies of precipitation, runoff, and land surface water storage change

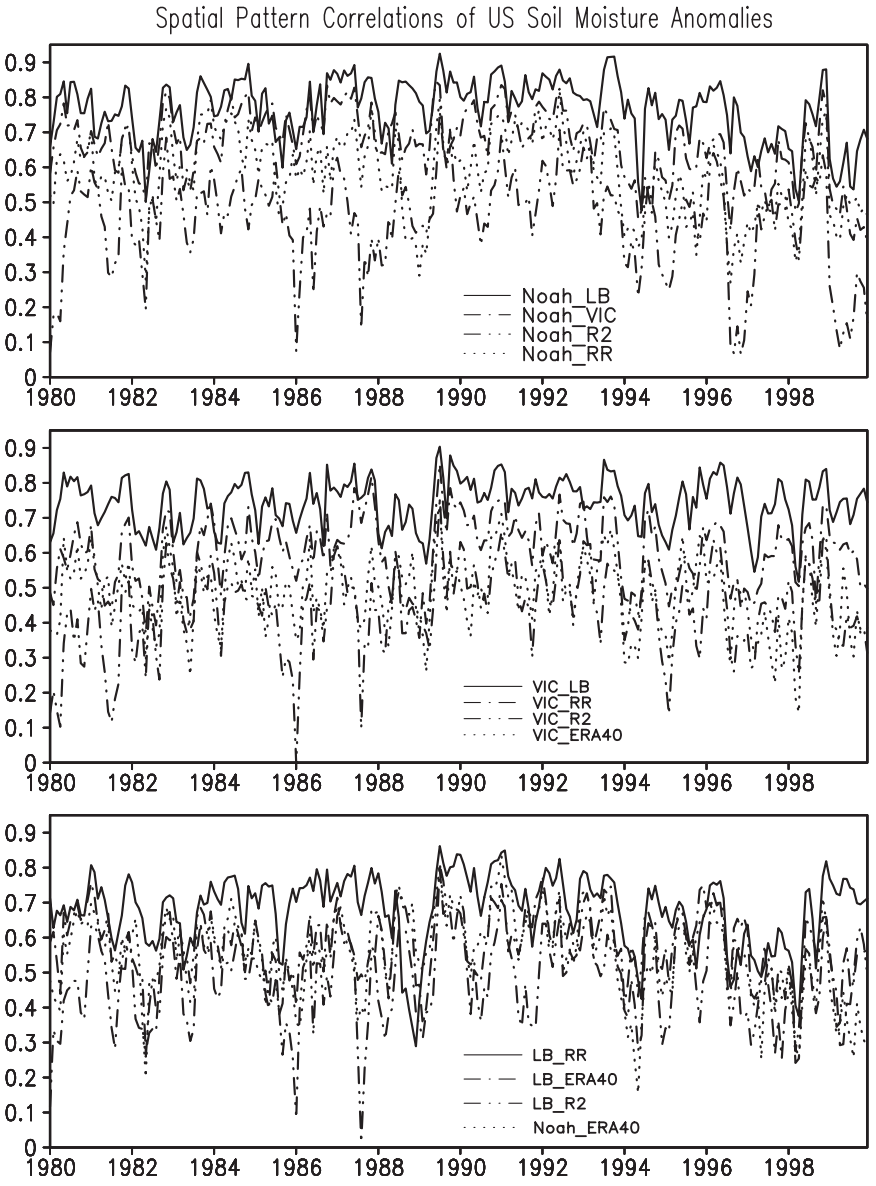

FIG. 14. Spatial pattern correlations of soil moisture anomalies over CONUS month by month for 1980–99. The legends (i.e., Noah_LB) refer to the correlations between the two (Noah and LB) datasets.

have similar magnitudes similar to their annual cycles and they are also closely related to one another. However, the E anomalies are relatively small, compared to other water budget components. This indicates that the interannual variations of land surface water storage changes are largely driven by interannual variations of precipitation, modulated by the interannual variations of runoff.

The analysis of spatial–temporal features of the simulated soil moisture reveals clear differences among different datasets, due to the differences of model physics, input forcing, and the mode of running (interactive or offline). The differences among datasets vary with time. In general, the spatial–temporal variability of simulated soil moisture over the CONUS from three offline runs and RR, all forced with observed precipitation, is more similar to one another. However, the two global reanalyses, R2 and ERA-40, sometimes present quite different soil moisture variability and distributions. The results show that the six land surface data assimilation systems used here do have a certain ability to capture the worst droughts and floods, such as

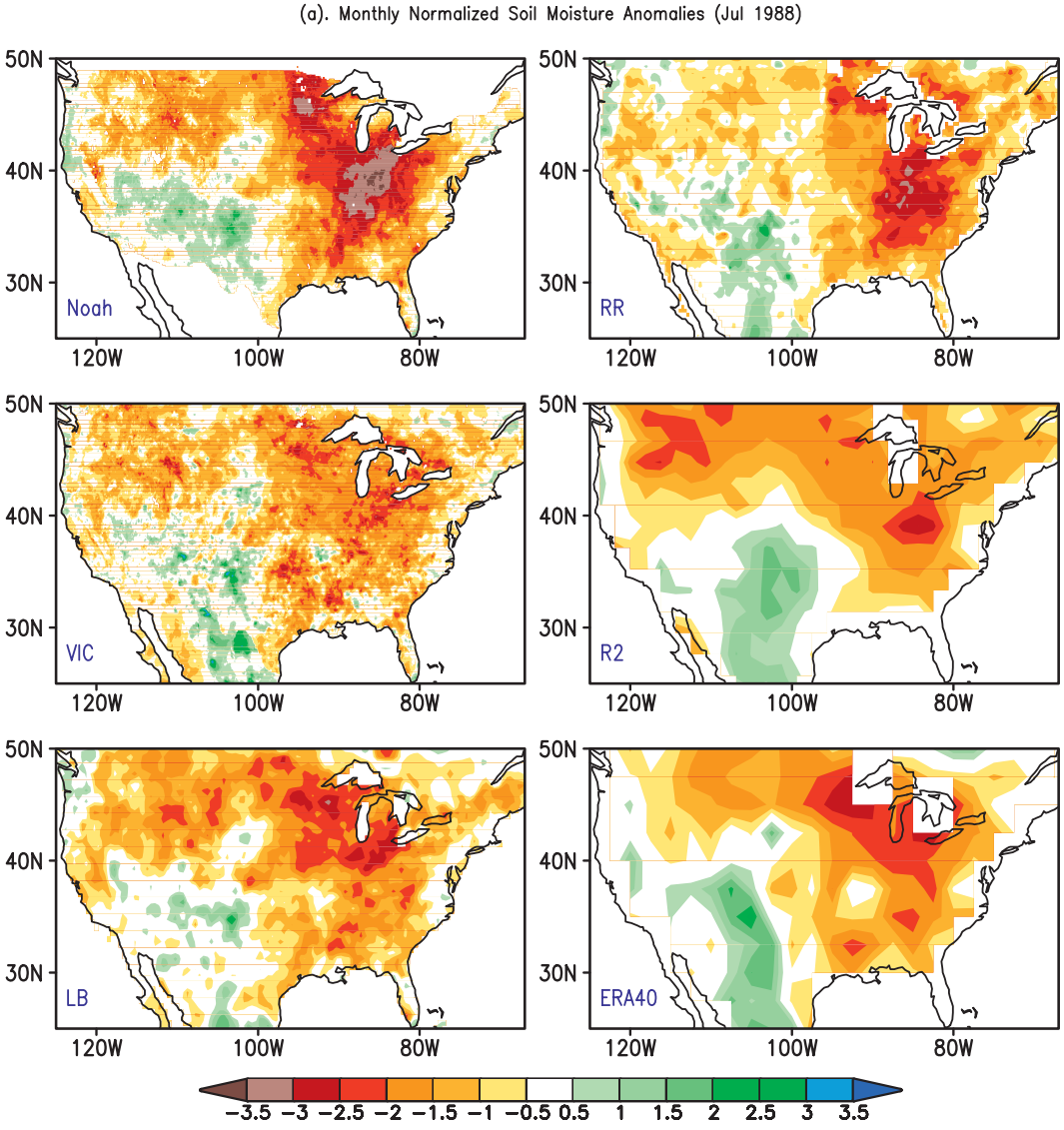

FIG. 15. (a) The simulated 1988 summer (July) drought from six land surface datasets. (b) The 1993 summer (July) flood from six land surface datasets. Soil moisture anomalies were normalized by dividing by their July standard deviations for 1980–99.

the 1988 summer drought and 1993 summer flood. In spite of the impressive similarity in model and experimental design, the RR and Noah runs have some surprising differences in outcomes, such as soil moisture, evaporation, and runoff standard deviations over the CONUS, which have to be caused by interactive (RR) versus offline (Noah) running.

Finally, in terms of overall performance of soil moisture simulation, the more comprehensive LSMs and reanalyses are no better than the very simplest system (i.e., LB in this set of models). However, to run these complicated LSMs (i.e., the Noah LSM and VIC LSM), seven forcing variables, namely, precipitation, air temperature, air humidity, surface pressure, wind speed, and surface downward shortwave and longwave radiation are needed, while LB only needs two variables (precipitation and surface air temperature) and is thousands of times cheaper to run than the complex systems. As of 2010, generating seven of these hourly forcing fields in real time and maintaining their spatial–temporal homogeneity over a multiyear period is still a huge challenge.

Acknowledgments. We thank Jesse Meng and Mark Rosencrans for internal review. We thank the hydrology group at the University of Washington and Research

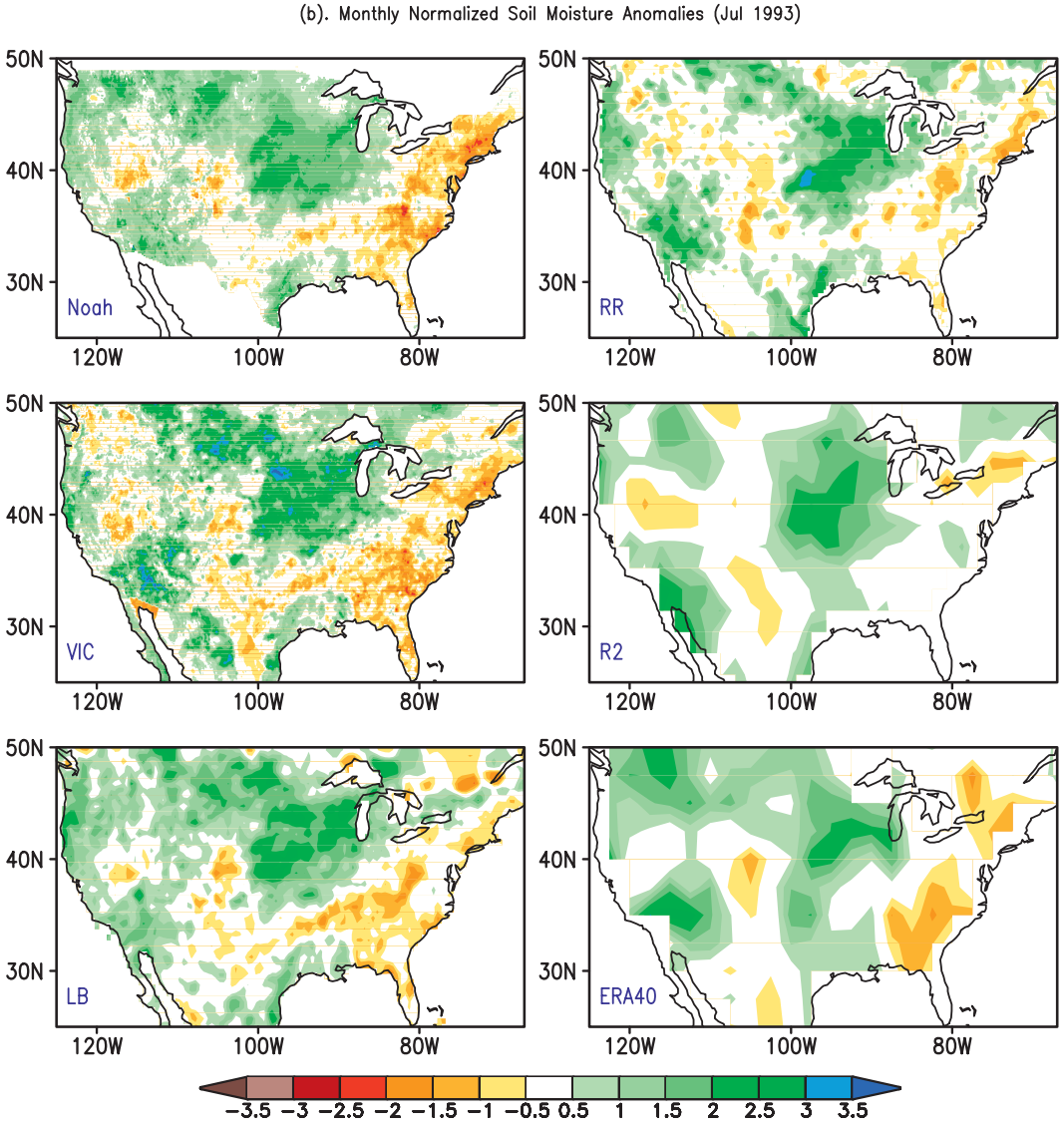

FIG. 15. (*Continued*)

Data Archive of NCAR for letting us download the VIC NLDAS run dataset and ERA-40 dataset. Thanks are also due to the two anonymous reviewers for their helpful comments and suggestions for improving the manuscript. This project was supported by GCIP Grant (GC00-095) and GAPP Grant (GC04-039).

REFERENCES

Chen, M., P. Xie, J. E. Janowiak, and P. A. Arkin, 2002: Global land precipitation: A 50-yr monthly analysis based on gauge observations. *J. Hydrometeor.,* **3,** 249–266.

Chen, T. H., and Coauthors, 1997: Cabauw experimental results from the Project for Intercomparision of Land-Surface Parameterization Schemes. *J. Climate,* **10,** 1194–1215.

Daly, C., R. Neilson, and D. Phillips, 1994: A statistical–topographic model for mapping climatological precipitation over mountainous terrain. *J. Appl. Meteor.,* **33,** 140–158.

Delworth, T., and S. Manabe, 1988: The influence of potential evaporation on the variabilities of simulated soil wetness and climate. *J. Climate,* **1,** 523–547.

Dirmeyer, P., 2000: Using a global soil wetness dataset to improve seasonal climate simulation. *J. Climate,* **13,** 2900–2922.

——, Z. Guo, and X. Gao, 2004: Comparison, validation, and transferability of eight multiyear global soil wetness products. *J. Hydrometeor.,* **5,** 1011–1033.

——, X. Gao, M. Zhao, Z. Guo, T. Oki, and N. Hanasaki, 2006: The Second Global Soil Wetness Project (GSWP-2): Multimodel analysis and implications for our perception of the land surface. *Bull. Amer. Meteor. Soc.,* **87,** 1381–1397.

Ek, M. B., K. E. Mitchell, Y. Lin, E. Rogers, P. Grunmann, V. Koren, G. Gayno, and J. D. Tarplay, 2003: Implementation of Noah

land-surface model advances in the NCEP operational mesoscale Eta model. *J. Geophys. Res.,* **108,** 8851, doi:10.1029/2002JD003296.

Fan, Y., and H. Van den Dool, 2004: The CPC global monthly soil moisture data set at ½ degree resolution for 1948-present. *J. Geophys. Res.,* **109,** D10102, doi:10.1029/2003JD004345.

——, and ——, cited 2005: Intercomparison of US land surface hydrologic cycles from multi-reanalyses and models. [Available online at http://www.cpc.ncep.noaa.gov/products/outreach/proceedings/cdw30_proceedings/cdpw_fan.ppt.]

——, and ——, 2008: A global monthly land surface air temperature analysis for 1948-present. *J. Geophys. Res.,* **113,** D01103, doi:10.1029/2007JD008470.

——, ——, D. Lohmann, and K. Mitchell, 2006: 1948–1998 U.S. hydrological reanalysis by the Noah land data assimilation system. *J. Climate,* **19,** 1214–1237.

Fennessy, M., and J. Shukla, 1999: Impact of initial soil wetness on seasonal atmospheric predictions. *J. Climate,* **12,** 3167–3180.

Hollinger, S. E., and S. A. Isard, 1994: A soil moisture climatology of Illinois. *J. Climate,* **7,** 822–833.

Huang, J., and H. M. Van den Dool, 1993: Monthly precipitation–temperature relations and temperature prediction over the United States. *J. Climate,* **6,** 1111–1132.

——, ——, and K. P. Georgakakos, 1996: Analysis of model-calculated soil moisture over the United States (1931–1993) and applications to long-range temperature forecasts. *J. Climate,* **9,** 1350–1362.

Kalnay, E., and Coauthors, 1996: The NCEP/NCAR 40-Year Reanalysis Project. *Bull. Amer. Meteor. Soc.,* **77,** 437–471.

Kanamitsu, M., W. Ebisuzaki, J. Woolen, S.-Y. Yang, J. Hnilo, M. Fiorino, and G. Potter, 2002: NCEP/DOE AMIP-II Reanalysis (R-2). *Bull. Amer. Meteor. Soc.,* **83,** 1631–1643.

——, C. Lu, J. Schemm, and W. Ebisuzaki, 2003: The predictability of soil moisture and near-surface temperature in hindcasts of the NCEP Seasonal Forecast Model. *J. Climate,* **16,** 510–521.

Kistler, R., and Coauthors, 2001: The NCEP–NCAR 50-Year Reanalysis: Monthly means CD-ROM and documentation. *Bull. Amer. Meteor. Soc.,* **82,** 247–267.

Koster, R. D., and M. J. Suarez, 2001: Soil moisture memory in climate models. *J. Hydrometeor.,* **2,** 558–570.

——, ——, R. W. Higgins, and H. M. Van den Dool, 2003: Observational evidence that soil moisture variations affect precipitation. *Geophys. Res. Lett.,* **30,** 1241, doi:10.1029/2002GL016571.

——, and Coauthors, 2004: Regions of strong coupling between soil moisture and precipitation. *Science,* **305,** 1138–1140.

——, Z. Guo, R. Yang, P. A. Dirmeyer, K. Mitchell, and M. J. Puma, 2009: On the nature of soil moisture in land surface models. *J. Climate,* **22,** 4322–4335.

Liang, X., D. P. Lettenmaier, E. Wood, and S. J. Burges, 1994: A simple hydrologically based model of land surface water and energy fluxes for general circulation models. *J. Geophys. Res.,* **99** (D7), 14 415–14 428.

Mahrt, L., and H. Pan, 1984: A two-layer model of soil hydrology. *Bound.-Layer Meteor.,* **29,** 1–20.

Maurer, E. P., G. M. O'Donnell, D. P. Lettenmaier, and J. O. Roads, 2001: Evaluation of the land surface water budget in NCEP-NCAR and NCEP-DOE reanalysis using an off-line hydrologic model. *J. Geophys. Res.,* **106** (D16), 17 841–17 862.

——, A. W. Wood, J. C. Adam, D. P. Lettenmaier, and B. Nijssen, 2002: A long-term hydrologically based dataset of land surface fluxes and states for the conterminous United States. *J. Climate,* **15,** 3237–3251.

Mesinger, F., and Coauthors, 2006: North America Regional Reanalysis. *Bull. Amer. Meteor. Soc.,* **87,** 343–360.

Mitchell, K. E., and Coauthors, 2004a: NECP completes 25-year North American Reanalysis: Precipitation assimilation and land surface are two hallmarks. *GEWEX News,* No. 14, International GEWEX Project Office, Silver Spring, MD, 9–12.

——, and Coauthors, 2004b: The multi-institution North American Land Data Assimilation System (NLDAS): Utilizing multiple GCIP products and partners in a continental distributed hydrological modeling system. *J. Geophys. Res.,* **109,** D07S90, doi:10.1029/2003JD003823.

Namias, J., 1952: The annual course of month-to-month persistence in climatic anomalies. *Bull. Amer. Meteor. Soc.,* **33,** 279–285.

Pan, H.-L., and L. Mahrt, 1987: Interaction between soil hydrology and boundary-layer development. *Bound.-Layer Meteor.,* **38,** 185–220.

Reed, C. D., 1925: Monthly forecasts by correlation. *Mon. Wea. Rev.,* **53,** 249–251.

Roads, J., and Coauthors, 2003: GCIP water and energy budget synthesis (WEBS). *J. Geophys. Res.,* **108,** 8609, doi:10.1029/2002JD002583.

Robock, A., K. Y. Vinnikov, G. Srinivasan, J. K. Entin, S. E. Hollinger, N. A. Speranskaya, S. Liu, and A. Namkhai, 2000: The Global Soil Moisture Data Bank. *Bull. Amer. Meteor. Soc.,* **81,** 1281–1299.

Rodell, M., and Coauthors, 2004: The Global Land Data Assimilation System. *Bull. Amer. Meteor. Soc.,* **85,** 381–394.

Rogers, E., M. Ek, Y. Lin, K. Mitchell, D. Parrish, and G. DiMego, cited 2001: Changes to the NCEP Meso Eta Analysis and Forecast System: Assimilation of observed precipitation, upgrades to land-surface physics, modified 3DVAR analysis. [Available online at http://www.emc.ncep.noaa.gov/mmb/mmbpll/spring2001/tpb.]

Schaake, J. C., and Coauthors, 2004: An intercomparison of soil moisture fields in the North American Land Data Assimilation System (NLDAS). *J. Geophys. Res.,* **109,** D01S90, doi:10.1029/2002JD003309.

Schaefer, G. L., and R. F. Paetzold, 2001: SNOTEL (SNOwpack TELemetry) and SCAN (Soil Climate Analysis Network). *Proc. Int. Workshop on Automated Weather Stations for Applications in Agriculture and Water Resources Management,* AGM-3 WMO/TD 1074, Lincoln, NE, WMO, 187–194.

Sellers, W. D., 1965: *Physical Climatology*. University of Chicago Press, 272 pp.

Torrence, C., and G. P. Compo, 1998: A practical guide to wavelet analysis. *Bull. Amer. Meteor. Soc.,* **79,** 61–78.

Uppala, S. M., and Coauthors, 2005: The ERA-40 Re-Analysis. *Quart. J. Roy. Meteor. Soc.,* **131,** 2961–3012.

Van den Dool, H., 2007: *Empirical Methods in Short-Term Climate Prediction*. Oxford University Press, 215 pp.

——, J. Huang, and Y. Fan, 2003: Performance and analysis of the constructed analogue method applied to US soil moisture over 1981-2001. *J. Geophys. Res.,* **108,** 8617, doi:10.1029/2002JD003114.

——, Y. Fan, J. Wahr, and S. Swenson, cited 2004: Gravity satellite data and calculated soil moisture: A mutual validation. [Available online at http://www.cpc.ncep.noaa.gov/products/outreach/proceedings/cdw29_proceedings/P3.19.ppt.]

Van den Hurk, B., 2002: European LDAS established. *GEWEX News,* No. 2, International GEWEX Project Office, Silver Spring, MD, 9.

——, J. Ettema, and P. Viterbo, 2008: Analysis of soil moisture changes in Europe during a single growing season in a new ECMWF soil moisture assimilation system. *J. Hydrometeor.,* **9,** 116–131.

Vautard, R., and Coauthors, 2007: Summertime European heat and drought waves induced by wintertime Mediterranean rainfall deficit. *Geophys. Res. Lett.,* **34,** L07711, doi:10.1029/2006GL028001.

Wahr, J., S. Swenson, V. Zlotnicki, and I. Velincogna, 2004: Time-variable gravity from GRACE: First results. *Geophys. Res. Lett.,* **31,** L11501, doi:10.1029/2004GL019779.

Wu, W., M. Geller, and R. Dickinson, 2002: The response of soil moisture to long-term variability of precipitation. *J. Hydrometeor.,* **3,** 604–613.

Yeh, T.-C., 1989: Sensitivity of climate model to hydrology. *Understanding Climate Change,* A. Berger, R. E. Dickinson, and J. W. Kidson, Eds., Amer. Geophys. Union, 100–108.

Zhang, H., and C. S. Frederikson, 2003: Local and nonlocal impacts of soil moisture initialization on AGCM seasonal forecasts: A model sensitivity study. *J. Climate,* **16,** 2117–2137.